Journal of Physiology (1989), **416**, *pp.* 183–213
With 13 *text-figures*
Printed in Great Britain

DEVELOPMENT OF Y-AXON INNERVATION OF CORTICAL AREA 18 IN THE CAT

BY MICHAEL J. FRIEDLANDER AND KEVAN A. C. MARTIN*

*Neurobiology Research Center and Department of Physiology and Biophysics, University of Alabama at Birmingham, Birmingham, AL 35294, USA and *MRC Anatomical Neuropharmacology Unit, Department of Pharmacology, Oxford University, Oxford OX1 3QT*

(*Received 22 December 1988*)

SUMMARY

1. Geniculocortical Y-axons ($n = 38$) in the optic radiations of 4–5-week-old kittens ($n = 20$) and adult cats ($n = 18$) were studied both physiologically and morphologically. Axons were recorded from intracellularly and subsequently filled ionophoretically with horseradish peroxidase (HRP). The HRP filled the axons' terminal arborizations in visual cortex (particularly well for those innervating area 18). Fourteen axons appeared to be completely filled with HRP ($n = 8$ in kitten, $n = 6$ in adult) and served as the basis for the quantitative analysis of the terminal arborizations reported in this study.

2. The distribution and correspondence of the axonal boutons to presynaptic elements in cortical layer 4A was analysed at both the light and electron microscope level using computerized three-dimensional analysis and serial section reconstruction, respectively. Compared to adult axons, the boutons of the kitten axons were smaller ($\bar{x} = 0{\cdot}75$ *vs.* $1{\cdot}75$ μm length, $P < 0{\cdot}001$) and more densely spaced both along individual axon branches ($\bar{x} = 6{\cdot}60$ *vs.* $11{\cdot}20$ μm interbouton interval, $P < 0{\cdot}001$) and between neighbouring branches of the same axon ($\bar{x} = 4{\cdot}7$ *vs.* $6{\cdot}4$ μm nearest-neighbour distance, $P < 0{\cdot}01$).

3. Most kitten boutons made a single Gray's type 1 synapse on a cortical neurone, unlike adult boutons which usually contacted two or more postsynaptic targets. Both kitten and adult axons had dendritic spines as their major target. Occasionally, HRP reaction-product was observed in cortical neurones postsynaptic to the labelled geniculocortical axon, which gave some estimate of the number of synaptic contacts between a single geniculocortical axon and target cell (about five).

4. The kitten Y-axons innervated the visual cortex in a pattern similar to that of the adult, with the richest terminal branching and bouton density in layer 4A with some additional boutons distributed in layers 3, 4B and 6. The extent of the terminal arborizations primarily in layer 4A (as measured in surface views) of kitten Y-axons in area 18 was significantly less than that of adult Y-axons in area 18 ($\bar{x} = 0{\cdot}9$ mm^2 *vs.* $\bar{x} = 1{\cdot}2$ mm^2, $P = 0{\cdot}04$).

5. We conclude that between 4 and 5 postnatal weeks and 1 year, geniculocortical Y-axons projecting to cortical area 18 undergo four major changes. These include a

reduction in synaptic bouton density (both in three-dimensional space and along individual branches), a concomitant moderate expansion in the surface area of cortex innervated, an increase in bouton size and an increase in the number of synaptic contacts made by each bouton. A general proportional growth of the individual axons' terminal arborization together with fusion and/or separation of neighbouring boutons is sufficient to explain this development.

INTRODUCTION

The visual cortex of the cat receives a major thalamic input via the parallel W-, X- and Y-cell pathways that originate in the retina and are distributed by the dorsal lateral geniculate nucleus (LGN_d; see Sherman & Spear, 1982; Sherman, 1985; and Friedlander (1988) for reviews). The most dense geniculocortical innervation is to layers 4 and 6 from the LGN_d X- and Y-cell pathways (LeVay & Gilbert, 1976; Gilbert & Wiesel, 1979; Freund, Martin & Whitteridge, 1985*a*; Freund, Martin, Somogyi & Whitteridge, 1985*b*; Humphrey, Sur, Ulrich & Sherman, 1985*a*, *b*). The parallel nature of this innervation is represented by the preference of many of the X- and Y- geniculocortical axon terminals for different sublaminae of layer 4 within area 17 of visual cortex (Gilbert & Wiesel, 1979; Freund *et al.* 1985*a*, *b*; Humphrey *et al.* 1985*a*, *b*) and a differential distribution of X- and Y-axons to various areas of cerebral cortex. The geniculocortical X-axons innervate only area 17 while the Y-axons innervate area 17 and area 18 (Stone & Dreher, 1973; Henderson, 1982; Freund *et al.* 1985*a*, *b*; Humphrey *et al.* 1985*a*, *b*; but see Ferster, 1987).

The X-cell-dominated geniculostriate pathway (to cortical area 17) has served as a useful system with which to study the processes of cortical development including synaptogenesis (Cragg, 1975), maturation of synaptic function (Tsumoto & Suda, 1982), the parcellation of territory by ingrowing geniculocortical afferents (LeVay, Stryker & Shatz, 1978; Shatz & Luskin, 1986; Stryker & Harris, 1986) and the emergence of receptive field (RF) organization (Hubel & Wiesel, 1963; Barlow & Pettigrew, 1971; Blakemore & Van Sluyters, 1975; Buisseret & Imbert, 1976; Bonds, 1979; Derrington & Fuchs, 1981; Albus & Wolf, 1984; reviewed in Fregnac & Imbert, 1984; Braastadt & Heggelund, 1985). Although recent reports have described the postnatal development of receptive field properties of neurones in cortical area 18 (Blakemore & Price, 1987; Milleret, Gary-Bobo & Buisseret, 1988), little is known of the structural development of this cortical area and its major thalamic input. This lack of information is surprising since area 18 offers several distinct advantages for understanding the ontogeny of visual processing and of general cerebral cortex development. These advantages include: (1) area 18 (layer 4) is innervated by a single functional class of LGN_d cell. Since layer 4 of area 18 receives only Y-cell innervation, the mechanisms controlling development may be less complex than in area 17 where a mixed and partially overlapping innervation of layer 4 by X- and Y-cells occurs. Thus, the establishment of synaptic sites is likely to be dominated by competitive binocular influences between Y-axons originating from adjacent LGN_d layers (Hubel & Wiesel, 1965; Hubel, Wiesel & LeVay, 1977) and not affected by

competition between functional cell classes. (2) The development of the Y-cell pathway is particularly sensitive to environmental influences during postnatal development (Sherman, Hoffman & Stone, 1972; Friedlander, Stanford & Sherman, 1982; Sur, Humphrey & Sherman, 1982; Friedlander & Stanford, 1984). The structural basis of this plasticity may be evident in the development of the Y-cell geniculocortical innervation. (3) The arborizations of Y-axons are highly divergent from retina through LGN_d to visual cortex (Friedlander, Lin, Stanford & Sherman, 1981; Sur & Sherman, 1982; Winfield & Powell, 1983; Freund *et al.* 1985*a*, *b*; Humphrey *et al.* 1985*a*, *b*) resulting in $\approx 5\%$ of the retinal ganglion cells (Stone, 1983) dominating $> 50\%$ of all geniculocortical synapses in layer 4 of areas 17 and 18 combined (Freund *et al.* 1985*b*).

At the retinogeniculate level, the Y-cells develop postnatally by a process of expansion of individual axon arborizations (Sur, Weller & Sherman, 1984; Friedlander, Martin & Vahle-Hinz, 1985). Does a similar process occur at the geniculocortical level or does the Y-innervation of area 18 develop by a retractive process as has been suggested for the geniculocortical innervation of area 17 (LeVay *et al.* 1978) and for a variety of other projections to kitten visual cortex (Innocenti, Fiore & Cemoniti, 1977; Koppel & Innocenti, 1983; Price & Blakemore, 1985)?

We evaluated the development of the geniculocortical Y-axon innervation to area 18 by combining electrophysiological, quantitative morphological and ultrastructural analysis of individual axons that were filled with horseradish peroxidase (HRP) by intracellular injection in 4–5-week-old kittens and adult cats. The kittens' age corresponds to a period when the Y-cell pathway from the retina to the LGN_d is still expanding (Sur *et al.* 1984; Friedlander *et al.* 1985), the geniculocortical Y-cells are still functionally immature (Wilson, Tessin & Sherman, 1982; Mangel, Wilson & Sherman, 1983; Tootle & Friedlander, 1986, 1989) and the development of the geniculocortical Y-pathway is highly sensitive to environmental factors (see Sherman & Spear, 1982 for a review). This is also the age when total synaptic density (reported for kitten visual cortex area 17; Cragg, 1975) is at its peak and thus, it would be expected that if a process of retraction of geniculocortical axonal arborizations occurs it would be evident at the ages studied.

Our results show that between the ages of 4–5 weeks and adult the overall extent of the geniculocortical Y-axon arborizations within layer 4 of area 18 *increases* modestly. During this period the distance between neighbouring boutons on a single axon (both along and between axon branches) increases resulting in a concomitant thinning of the bouton density while the individual axon arbors expand. The individual boutons increase in size and the number of synaptic targets for each bouton also increases during this same period. We conclude that from the age of 4–5 weeks to adult, the development of the geniculocortical innervation of area 18 by Y-cells proceeds in a fashion similar to the retinogeniculate Y-cell projection and that the 'exuberance' of the thalamocortical projection is in terms of individual axons' bouton density, not in areal extent of the arborizations. Preliminary accounts of these findings have appeared (Friedlander, Martin & Tootle, 1984; Friedlander, Wilson, Martin, Fancher & Alones, 1986).

METHODS

Surgery and general preparation

Fifteen kittens and eleven adult cats were reared in our breeding colony. Ages and weights at experimentation were 30–37 days, 475–570 g and > 1 year, 2–3 kg for the kittens and adult cats, respectively. (The axons from two adult cats were also used as part of another study; Freund *et al.* 1985*a*, *b*). Animals were given a dose of atropine (0·02 mg kg^{-1}) subcutaneously to prevent excessive respiratory secretion. Anaesthesia was initially induced with halothane (Abbott; 1·0–1·5% in kittens, 3·0% in adult cats) in a 1:1 mixture of $N_2O:O_2$. Surgical procedures were carried out on a temperature-controlled blanket. The femoral vein was cannulated and the halothane discontinued. Anaesthesia for further surgical procedures was effected with alphaxalone/alphadalone (Saffan–Glaxovet) administered intravenously in a 2·4 mg ml^{-1} solution diluted in warmed physiological saline. The alphaxalone/alphadalone was administered as needed during surgery (range of doses administered = 15–20 mg kg^{-1}). The femoral artery was then cannulated and the cannula was connected to a Statham pressure transducer. Continuous records of blood pressure and heart rate were obtained throughout the experiment. Mean blood pressure was kept between 90–120 mmHg. The bladder was periodically voided by compression throughout the experiment. After tracheal cannulation, the animal was placed in a stereotaxic frame. The ear bars and wound margins were coated with a long-lasting, oil-based local anaesthetic (procaine base and butamben, Anduracaine; Reid Provident). The animal was paralysed with an initial dose of 20–40 mg kg^{-1} of gallamine triethiodide (Flaxedil, Davis & Geck) and mechanically ventilated. The inspired gases were changed to a 70:30 mixture of $N_2O:O_2$ and were continued in this fashion for the remainder of the experiment. Flaxedil administration was continued throughout the experiment with an infusion pump at a rate of 12·0 mg kg^{-1} h^{-1} in a 5% lactated Ringer solution. (The adults were supplemented with 0·25 mg kg^{-1} h^{-1} of *d*-tubocurarine.) Additional alphaxalone/alphadalone (0·5–2·0 mg kg^{-1} h^{-1}) was administered throughout the surgical procedures and during electrophysiological recording. The continuous monitoring of blood pressure and heart rate while periodically testing with ear and foot pad compression ensured that the animals remained well-anaesthetized. Expired P_{CO_2} was monitored with a Beckman LB-II CO_2 monitor and kept between 3·8–4·3%. Heart rate was kept below 200 beats min^{-1} in adult cats and 270 beats min^{-1} in kittens. If the animal showed any signs of stress throughout the remainder of the experiment (blood pressure or heart rate increases) the 70:30 mixture of $N_2O:O_2$ was supplemented with additional injections of alphaxalone/alphadalone.

Optics

The cats' pupils were dilated with 1% ophthalmic atropine sulphate (Alcon), the nictitating membranes were retracted with 10% phenylephrine hydrochloride (Neo-Synephrine, Winthrop) and the eyes were flushed with ophthalmic antibiotic (Neosporin, Burroughs Wellcome). The cats were fitted with plano contact lenses (base curvature range = 5·00–6·25 mm for kittens, 7·75–8·50 mm for adult cats). The appropriate lenses were fitted to make the animals' retinae conjugate with the stimulus display positioned at a viewing distance of either 171 or 57 cm. If additional optical correction was needed (after being determined by streak retinoscopy) appropriate spectacle lenses were placed in front of the eyes.

Electrodes

Bipolar electrodes were used for electrical stimulation of the optic chiasm (OX) and the optic radiations (OR). These electrodes were made of lacquer-coated tungsten wires insulated to within 0·5 mm of their tips. The OX-stimulating electrodes were positioned at Horsley–Clark (H–C) stereotaxic co-ordinates: anterior 9·0 mm, lateral 1·0 mm in kittens and anterior 15·0 mm, lateral 1·0 mm in adult cats. The optimum electrode depth for OX was determined by lowering the electrode while recording the evoked potential in response to 2·0 Hz stroboscopic illumination of the eyes. The electrodes were then cemented to the skull with dental cement. The OR-stimulating electrodes were positioned 2 mm above the LGN_d as determined by recording the evoked response to visual stimulation. Recording micropipettes (tip diameter = 0·2–0·5 μm) were filled with a

solution of 0·2 M-KCl, 0·05 M-Tris (Sigma) and 4·0% HRP (Sigma VI) at a pH of 7·0. The micropipettes were bevelled to final impedances of 90–140 MΩ at 200 Hz. Micropipettes were inserted into the OR at a 20 deg angle (lateral to the vertical axis) between H–C −4·0 to +3·0 mm. Axons of LGN_d cells were typically recorded at depths of 0·8–3·2 mm from the cortical surface (which usually corresponded to the white matter just below cortical layer 6).

Stimulus display and cell classification

Receptive fields of LGN_d cell axons were initially plotted with flashing spots on a tangent screen at a viewing distance of 171 cm. Subsequent testing was done with a Tektronix model 608 (phosphor P 31) display monitor positioned at a viewing distance of 57 cm (screen area = 10 deg × 10 deg). Flashing spots or sinusoidally counterphased, spatially sinusoidal vertical gratings were generated on the display monitor by a Picasso Image Generator (Innisfree, USA). Axons of LGN_d cells were tested for several properties. These included: (1) ocular dominance; (2) receptive field centre position, size and contrast sign (measured qualitatively by listening to an audio monitor to evaluate the vigour of the axon's response to manually controlled light flashes of 2 s duration); (3) presence of an inhibitory surround region (evaluated by comparing the axon's response to a spot of appropriate contrast that just filled the receptive field centre with an equal luminance spot which was 5 times as large as the centre); (4) linearity of spatial summation to a counterphased, vertical sinusoidal grating (mean luminance = 32 cd m^{-2}, counterphase rate = 0·5–2·0 Hz, spatial frequency appropriately high to reveal the second harmonic of the cell's response); responses were considered non-linear if the axon's modulated response had a discernible second harmonic component (see Tootle & Friedlander (1986, 1989) for consideration of this analysis for kitten LGN_d neurones). In cases where the linearity of the cell's response was not clearly identifiable by listening, the cell's response to grating counterphase at several phase positions was collected under computer control. The summed responses over 50–100 trials were subjected to Fourier analysis. If the ratio of the second harmonic response amplitude/fundamental amplitude was > 2·0, the cell's response was considered non-linear; (5) responsiveness to a rapidly moving (> 200 deg s^{-1}) large (12 deg × 12 deg) target of contrast opposite to that of the receptive field centre sign (adult Y-axons typically responded reliably with an increased firing rate each time this stimulus was moved through their receptive field), (6) latency to suprathreshold electrical stimulation of the optic chiasm and optic radiations at 1 Hz (measured from the onset of the stimulus artifact to the beginning of the action potential), and (7) the regularity and temporal jitter of the response to electrical stimulation.

Axons were considered to originate from LGN_d Y-cells in adult cats if they responded to grating counterphase with a phase-independent doubling response indicative of non-linear spatial summation (see Fig. 1), their latency to electrical stimulation of the optic chiasm was < 2·0 ms (or the OX–OR latency difference when both responses were obtained was < 1·5 ms) and they responded reliably to high velocity visual stimuli (see criteria (5)). This battery of tests is a reliable indicator of LGN_d Y-cells in adult cats (Friedlander & Stanford, 1984). In the kitten, the criteria for separating LGN_d X- from Y-cells are less conclusive. However, we have recently demonstrated that the presence of non-linear spatial summation at 4–5 weeks of age is a reliable indicator for Y-cells (Tootle & Friedlander, 1989). This approach will only include Y-cells in our sample but may exclude some kitten axons that have not yet developed Y-cell physiological properties (since our previous studies indicate that errors in classifying kitten LGN_d neurones were primarily due to false negatives on testing for *non*-linear spatial summation and not the reverse situation; Tootle & Friedlander, 1986, 1989). The reliability of the approach was substantiated by the morphological results of this study in that kitten axons classified as Y-axons had essentially similar overall projection patterns and areal and laminar distributions to adult Y-axons (Freund *et al.* 1985*a*, *b*; Humphrey *et al.* 1985*a*, *b* and this study).

HRP injection and tissue processing

After the axon had been electrophysiologically characterized as an LGN_d axon, it was penetrated with the micropipette. The intra-axonal recording condition was indicated by a drop in the D.C. level to between −30 and −68 mV. The axon's receptive field properties were checked repeatedly throughout the intracellular recording which lasted from 5 to 20 min on average. The axon was then

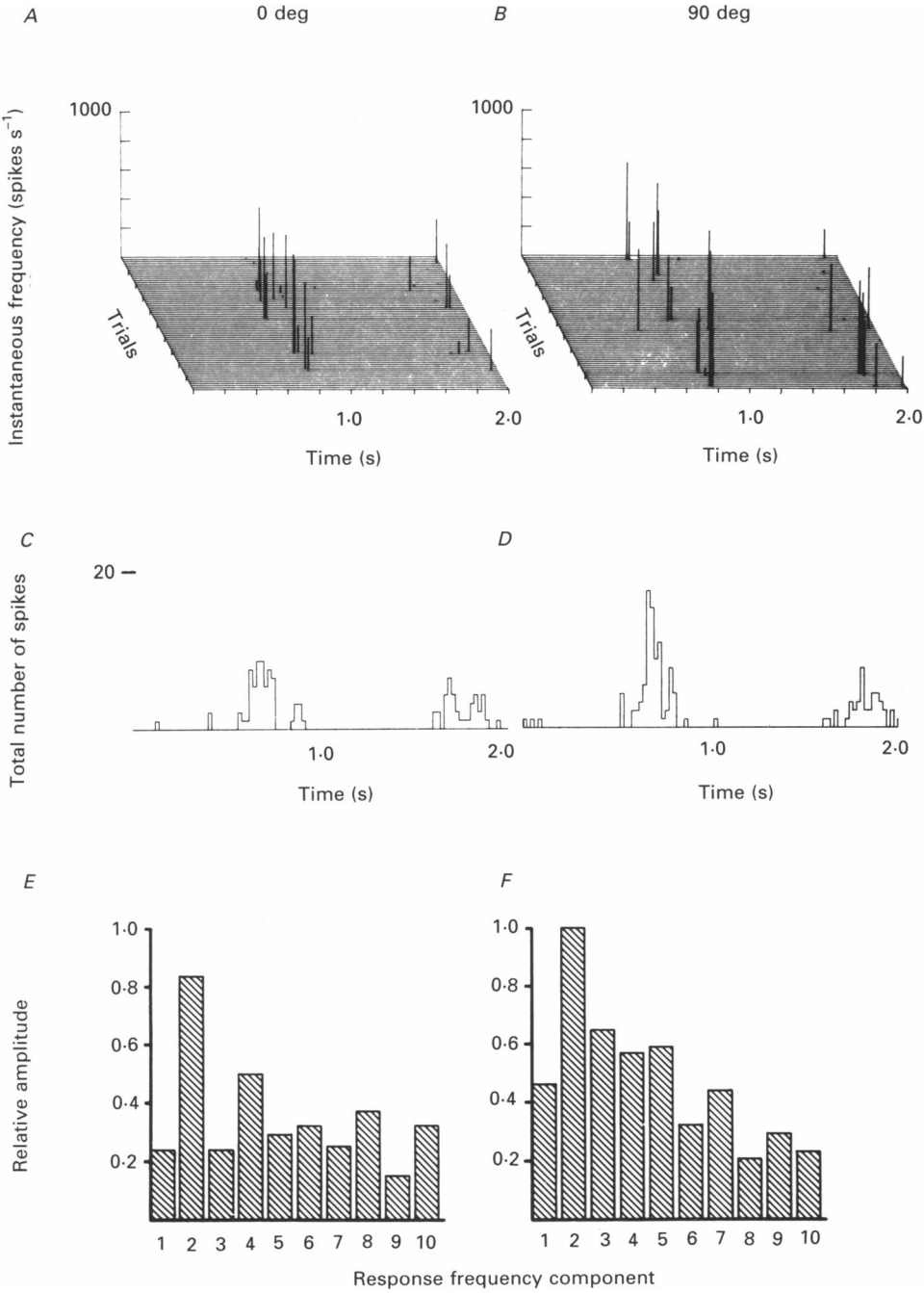

Fig. 1. Example analysis of a kitten geniculocortical Y-axon's response to sinusoidally counterphased grating pattern. Upper panels (*A* and *B*) and firing rate plots representing the axon's response on individual trials with the grating placed at two positions (0 and 90 deg). The vertical grating pattern was modulated at 0·5 Hz (spatial frequency = 1·2 cycles deg^{-1}) with a contrast (luminance$_{max}$ − luminance$_{min}$)/(luminance$_{max}$ + luminance$_{min}$) = 0·2. Note that a 'doubling response' characteristic of non-linear spatial summation occurred at both phase positions (as well as at two other phase positions (22·5

ionophoretically filled with HRP by passing depolarizing current pulses of 2·0–8·0 nA (200 ms duration at 2·5 Hz) from 3 to 25 min. The micropipette was then withdrawn and a new penetration was made. Only LGN_d axons that were impaled in the white matter and well-filled with HRP were included in this study since penetration of LGN_d axons within the cortical laminae may occur past axonal branch points and result in incomplete filling with HRP. Up to four axons were injected in each hemisphere. Injection sites were spaced by > 1 mm in the anterior–posterior (A–P) axis in order to identify reliably the HRP-injected axon from which the electrophysiological data were obtained. The animals were deeply anaesthetized with Nembutal from 2 to 24 h after the last axon was injected and perfused transcardially with heparinized saline followed by a modified Karnovsky's fixative (2·5% glutaraldehyde, 1·0% paraformaldehyde in phosphate buffer). The visual cortex was subsequently blocked in the coronal plane. Sections were cut on a Vibratome (Oxford Instruments) at 80 μm and tested for HRP activity with the catechol/p-phenylene reaction method of Hanker, Yates, Metz & Rustioni (1977) with cobalt and nickel intensification (Adams, 1981). Wet sections were examined for HRP-filled processes at 160 × and were post-fixed in osmium tetroxide (1% solution in 0·1 M-phosphate buffer for 45–60 min depending on the background darkness of the HRP reaction). The sections were dehydrated in ethanol (1% uranyl acetate was included in the 70% ethanol stage for 40 min), mounted on slides in Durcupan ACM resin (Fluka) under a cover-slip and cured for 2 days at 56 °C.

The osmication and embedding in plastic of the tissue proved to be advantageous for light microscopic (LM) analysis of the axonal structure (as well as the obvious benefit of facilitating further electron microscopical (EM) analysis of the same tissue). The shrinkage of the tissue orthogonal to the plane of section was greatly reduced (as compared to tissue that was treated for light microscopy by standard dehydration and clearing procedures). Section thickness (as measured to 0·5 μm accuracy with an optical encoder on the microscope stage) in the osmicated tissue was close to the original value at which it was cut (62–75 *vs.* 80 μm) compared to the severe shrinkage observed in tissue treated for LM with conventional processing methods (20–34 *vs.* 80 μm). This facilitated our three-dimensional analysis of the structure of the axons' terminal arborizations within the visual cortex. The shrinkage factor (6–23%) was incorporated into all subsequent measurements of bouton spacing and density based on measurements of each individual section analysed for the kittens and adults. The arborizations from selected osmicated sections were drawn under oil-immersion (40 or 50 × objectives), photographed through the light microscope, had their boutons' positions digitized and reconstructed in three-dimensional space (see below) and were re-embedded for correlated electron microscopy (see Freund *et al.* 1985*a*). Serial ultrathin sections were cut from the middle of selected axons' terminal arborizations in cortical layer 4A, mounted on Formvar-coated single slot grids and stained with uranyl acetate and lead citrate. Electron micrographs were taken at 80 kV with a 20 μm objective aperture on a JEOL 100 CX transmission electron microscope. Selected boutons (or interbouton segments) of the axons' terminal arborizations were observed with the LM and were subsequently examined with the EM

---

and 45 deg) not illustrated). This weak phase-independent doubling with large inter-trial variability in responsiveness was characteristic of many geniculocortical Y-axons in the kitten. The middle panels (*C* and *D*) illustrate the peristimulus time histograms (PSTHs) constructed by summing the individual trial responses to grating counterphase illustrated in *A* and *B*. Bin width = 10 ms. The lower panels (*E* and *F*) illustrate the Fourier analysis of the PSTHs shown above. The response power of components at the fundamental (equal to the counterphase frequency = 0·5 Hz) and sequential harmonics (up to and including the tenth harmonic) are normalized with respect to the component with the most power (in this case equal to the second harmonic at the 90 deg phase position). Note that the responses at both phase positions illustrated are considerable at the second harmonic (second harmonic/fundamental ratio > 2·0 for each phase position) meeting the criteria for non-linear spatial summation. It is of interest to note that many kitten geniculocortical Y-axons had considerably weaker second harmonic responses but had other physiological properties (and cortical projection patterns) indicative of Y-axons. However, we conservatively only included those with significant second harmonic responses in this study for comparing to the adult Y-axons. See Tootle & Friedlander (1989) for a detailed consideration of the classification of kitten Y-cells.

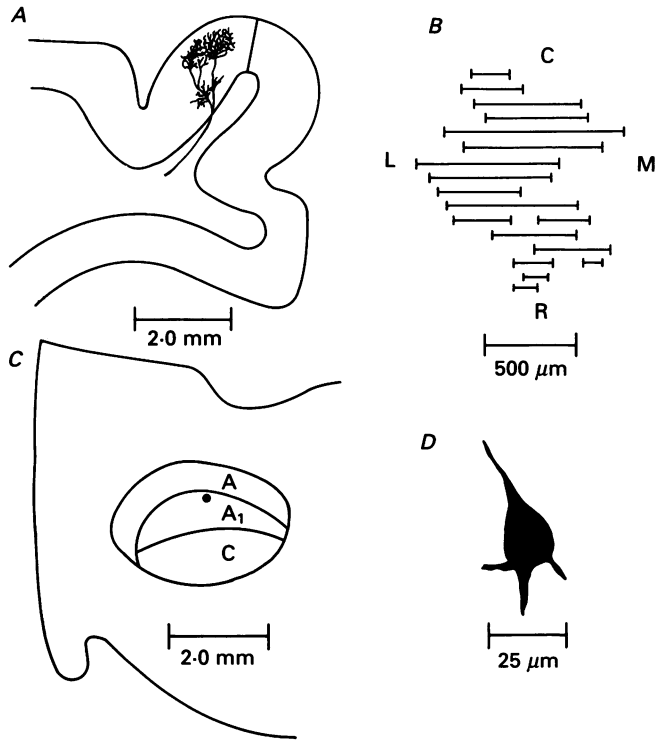

Fig. 2. Drawings of arborization extent and cell body of a kitten LGN_d Y-cell. Panel *A* is a *schematic* drawing of the location of the terminal arborization in cortical area 18. Line indicates the area 17/18 border. Panel *B* is a surface view of the visual cortex that illustrates the distribution of the axon's boutons located in layer 4 (with some in layer 3). The solid bars represent the width in the mediolateral axis of zones containing clumps of boutons in individual sections. Breaks in the bars represent regions of $\geqslant 100$ μm where no bouton occurred. Each level represents an individual 80 μm thick section. R = rostral, C = caudal, M = medial, L = lateral. Calculations of the surface area of the axon's innervation of cortical layer 4 (and 3) were derived from these chartings. The total surface area was taken as the sum of the product of section thickness (80 μm) and mediolateral extent of *only* the bouton-containing zones for serial sections. Thus, our measure of surface area is conservative and does not take into account total extent including bouton-free zones (see Humphrey *et al.* 1985*a*). Panels *C* and *D* illustrate the location and the shape of the LGN_d cell that gave rise to the axon illustrated. The cell was located and drawn by virtue of its being retrogradely filled with HRP after injecting the axon intracellularly in the cortical white matter. Geniculate layers are indicated A, A_1 and C.

in serial sections to determine the reliability of an observed bouton at the LM level corresponding to a site of synaptic contact (and conversely to the reliability of interbouton axon segments not corresponding to synaptic zones) in the kittens and adult cats.

In five kittens, the LGN_d was also blocked out, sectioned on a vibratome at 100 μm and reacted for HRP histochemistry as described above. This was done to locate the retrogradely labelled LGN_d cells-of-origin of the geniculocortical axon arborizations that were recovered in visual cortex. This method only proved successful for three of five of the kitten axons analysed in this report. Two of their cell bodies were located in LGN_d lamina A_1 and one occurred in lamina A (see Fig. 2). The soma sizes were consistent with those of Y-cells for kittens of this age (Friedlander, 1982, 1984). However, the dendritic morphology was not apparent from the retrograde fills to relate the data obtained from direct intrasomatic injections of HRP into LGN_d Y-cells (Friedlander *et al.* 1981; Friedlander, 1982).

Analysis of axons' terminal arborizations

Qualitative analysis

The HRP-filled axons were drawn from each section and reconstructed as two-dimensional montages. Axons were selected for drawing and further quantitative analysis only if: HRP injections were made in the white matter, the injections were clearly into a single axon (as determined by inspection of the injection site), axonal branches were darkly filled with clearly visible boutons along their course (as viewed at 160 × magnification), the HRP reaction-product in branches was not seen to fade over distance and branches could be followed towards end-like structures (terminal clusters of boutons or a narrowing of the axon segment). While reconstructions of entire axons' terminal arborizations were made from drawings at 400–500 ×, selected sections were drawn at 1200 × to make size measurements of individual boutons in kittens and adult cats.

The extent of the boutons in layers 3 and 4 were measured by constructing surface view drawings of their distribution in serial sections. The areal extent of the bouton distribution in an individual section was taken as the product of section thickness (80 μm in the anterior–posterior axis) and the extent of the layer 3 and 4 boutons in the mediolateral (ML) axis, excluding regions that were free of clumps of boutons for $\geqslant 100$ μm. The *total* surface area of an arborization was expressed as the sum of these areas from the serial sections through the reconstructed length of the arborization (see Fig. 2). Location of the axons' terminal arborizations was determined according to the cytoarchitectonic criteria of Hubel & Wiesel (1965). Subdivision of cortical lamina 4 into dorsal and ventral tiers (4A and 4B, respectively) was according to the criteria of O'Leary (1941) and Lund, Henry, MacQueen & Harvey (1979). The lamination is readily visible in the osmicated material in the kittens and adult cats. The areal borders of visual cortex (particularly the boundary between areas 17 and 18) are clear in the osmicated material from adult cats. This division is slightly less distinct in the kitten. (A recent report by Price & Blakemore (1985) indicates that staining for cytochrome oxidase facilitates these areal distinctions in the neonate although this was not attempted in the present study.)

Quantitative analysis

After the terminal arborizations were drawn, the region of the axon's innervation of layer 4 was selected from the centre of the arborization for quantitative analysis of bouton distribution. This region was selected to allow normalization of the bouton densities for comparison between axons. Moreover, although the axons used for quantitative analysis were well-filled with HRP reaction-product, by confining our quantitative measurements to the centre of the arbors, even the slight possibility of missing any boutons was reduced. This region was approximately 1·00 mm wide × 0·50 mm high × 0·08 mm thick for each of three to four serial sections. The position of each bouton along the axonal branches in this region was digitized (at 500 ×, resolution = 0·5 μm) with the use of software developed in our laboratory to run on a PDP 11/23 computer and a microscope equipped with optical encoders to read stage position (X- and Y-axes), a digitizing tablet with a microscope drawing tube attachment to encode position within a field of view and optical encoding of focal depth (Z-axis). The distribution of the boutons was visualized from a variety of perspectives using an image rotation program developed in our laboratory that runs on a DEC VAX 11/750 computer and an Evans & Sutherland PS-300 graphics work station.

The interbouton interval (IBI) measurements were calculated by an algorithm that uses the X, Y and Z co-ordinates of each bouton to calculate the vector to the adjacent bouton on that axon branch. Thus, the IBIs reflect the shortest direct path (in three-dimensional space) between neighbouring boutons. By identifying each bouton's location on the axon as each point is entered (with respect to it being on a given branch, first bouton, bouton-of-passage, terminal bouton, etc.) the IBI analysis is done only for neighbouring boutons-of-passage on an axonal branch (*vs.* spacing between boutons on one branch and those on another branch). The distribution of boutons in three-dimensional space with respect to neighbouring boutons on either the same or other branches was analysed by two methods. The first simply calculated the average density of boutons as the number per unit volume of cerebral cortex, bounded by the most extremely positioned boutons in the region analysed. These density measures should only be considered as averages and obviously do not reflect the heterogeneous clustering of the boutons of a single axon in the three-dimensional cortical matrix. The second method employed a form of nearest-neighbour analysis modified for use

in three-dimensional space. The distance from each bouton to its nearest neighbour (calculated as a direct vector, as for the IBI measurements, except that the nearest neighbour could be located either on the same branch or a neighbouring branch) was calculated and plotted as a frequency distribution histogram. The nearest-neighbour values of the extreme points (boutons) in each plane were omitted from analysis in each section.

Unless otherwise specified, all statistical comparisons were made with a Mann–Whitney U test.

RESULTS

General

We recorded extracellularly from thirty-four adult and fifty-two kitten geniculocortical axons that were characterized as emanating from LGN_d Y-cells based on the battery of electrophysiological tests described in Methods. Most of these were subsequently impaled with a micropipette and had HRP infused ionophoretically into them for periods of time from a few seconds to 20 min. A total of eighteen Y-axons from adult cats and twenty Y-axons from kittens were sufficiently well-filled with HRP to allow qualitative analysis of their projection pattern and the distribution of their terminal arborization at the light microscope level. Of these, six adult Y-axons (from five cats) and eight kitten Y-axons (from six kittens) projecting to area 18 were labelled particularly heavily and satisfied all of our criteria (described in Methods) for complete filling to allow quantitative analysis of the distribution of their boutons within layer 4 of visual cortex. These fourteen axons from eleven animals form the basis for the quantitative analyses and conclusions presented in this report. Five axons (two adult axons from a previous study (Freund *et al.* 1985*a*,*b*) and one additional adult axon from this study and two kitten axons) were further analysed at the electron microscope level.

Electrophysiology

Figure 1 shows an example of the results of our electrophysiological characterization of one of the kitten Y-axons projecting to area 18 that was also successfully injected with HRP. The response of this cell to grating counterphase on each of seventy trials is illustrated for the two spatial phase positions indicated in Fig. 1*A* and *B*. Note that the cell's response to this stimulus varied considerably on a trial by trial basis. This lability of the non-linear 'doubling' response is common in many kitten Y-cells (both in LGN_d, Friedlander, 1982; Mangel *et al.* 1983; Tootle & Friedlander, 1986, 1989; and in retina, Sur *et al.* 1984; Friedlander *et al.* 1985; Friedlander & Tootle, 1988; Tootle & Friedlander, 1989). The summed responses over all trials are shown as peristimulus time histograms (PSTH) in Fig. 1*C* and *D*. The phase independence (see Hochstein & Shapley, 1976*a*, *b*) of the cells' response is apparent. These PSTHs were subsequently analysed by the Fourier method. These results are illustrated in Fig. 1*E* and *F*. Note the relative amplitude of the second harmonic response component at both stimulus phase positions (second harmonic/fundamental response ratio at 0 deg = 3·6, second harmonic/fundamental response ratio at 90 deg = 2·3). Also, note the relative strengths of the additional even harmonic characteristic of a Y-cell's non-linear response. The additional harmonic distortion is considerable due to the responses' transient and sinusoidal forms.

Reconstructed drawings of axonal arborizations

Figure 3*A* and *B* shows the appearance of example adult and kitten Y-axons projecting to area 18. The adult axon, previously illustrated in Freund *et al.* (1985*a*) is shown again here because it has similar physiological properties and it occupies a similar portion of the post-lateral gyrus to the kitten axon. The kitten axon is the

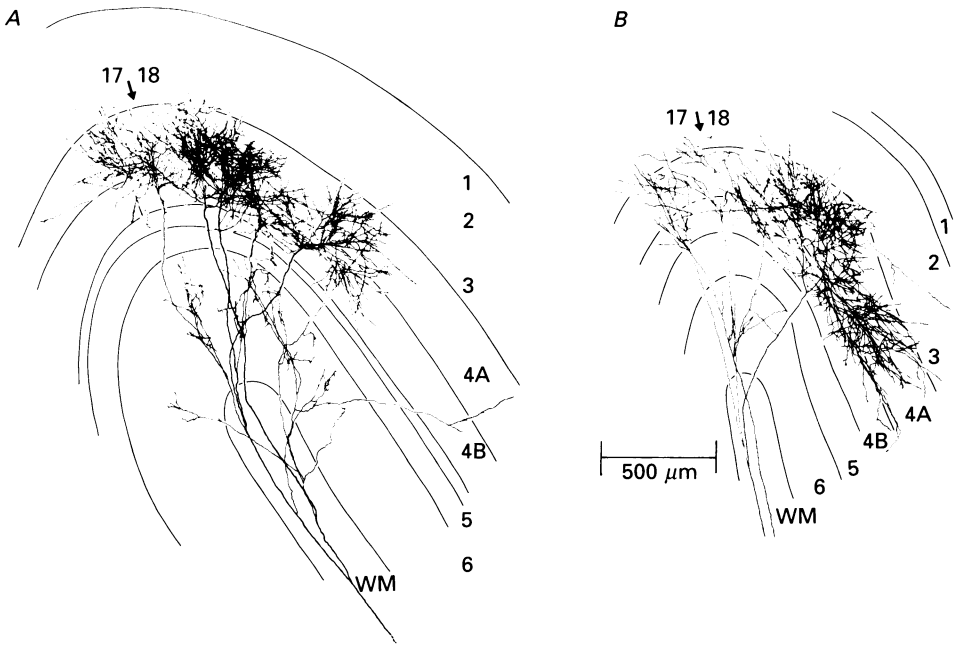

Fig. 3. Drawings of adult (*A*) and kitten (*B*) geniculocortical Y-axon terminal arborizations which predominantly innervate area 18 (area 17/18 border is indicated by arrows). Both axons had on-centre receptive fields and exhibited non-linear spatial summation to a counterphased grating stimulus as illustrated in Fig. 1. Receptive field centre sizes and response latency to electrical stimulation of the optic chiasm were 0·8 deg, 1·1 ms and 2·5 deg, 1·9 ms for the adult and kitten axons, respectively. Receptive field locations are given in the text. Scale bar = 500 μm. WM, white matter.

same one from which the electrophysiological records illustrated in Fig. 1 were obtained. Both axons show variations in the density of their innervation of layer 4. In this view the clusters appear denser in the adult, but this is because the adult axon is larger and hence more axonal processes have been collapsed into two dimensions. The laminar distribution of boutons is similar in adult and in kitten. About 30–40% of the boutons are found in layer 4B in the kitten, as was found for the adult (Freund *et al.* 1985*a*).

Correlation of boutons with synaptic specializations

Before beginning the detailed analysis of the axons it was necessary to establish that the boutons seen at the light microscope level were indeed sites of synaptic

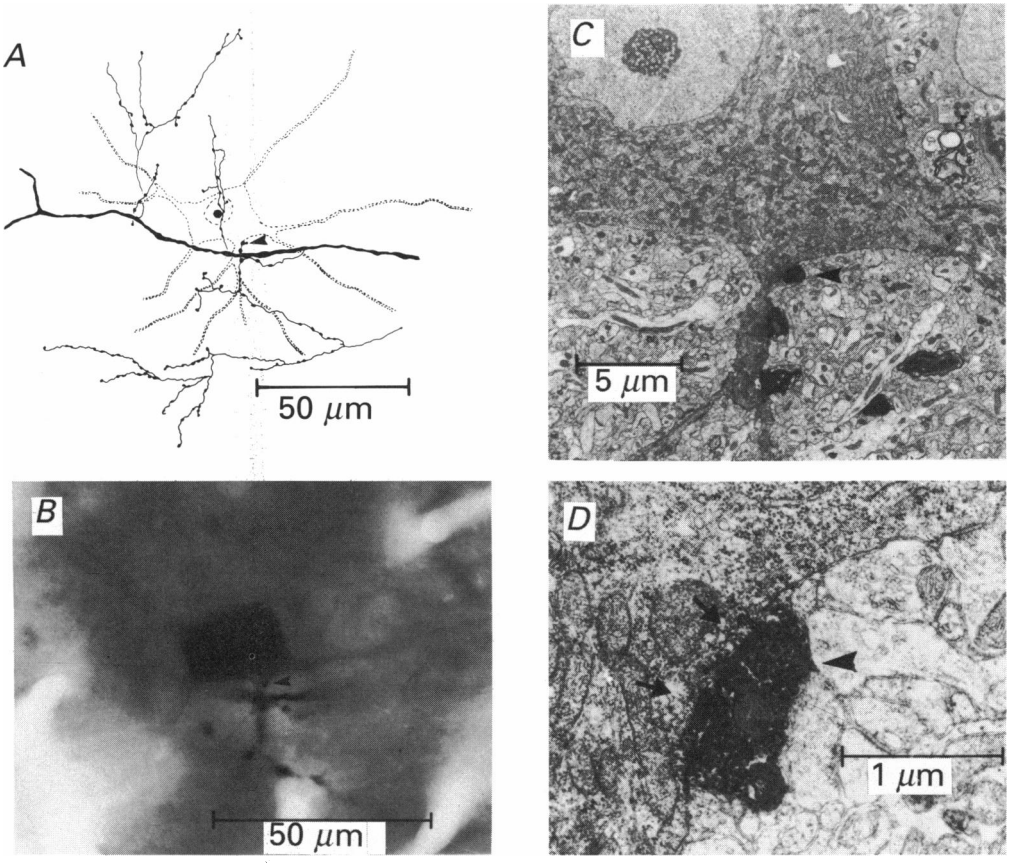

Fig. 4. Example of correlated light and election microscopy of part of HRP-filled terminal arborization of kitten geniculocortical Y-axon innervating area 18. Axon is same as that illustrated in Fig. 2*B*. Figures also demonstrate trans-synaptic filling of single layer 4A cortical target neurone from innervating boutons of the geniculocortical axon. *A*, drawing of part of central terminal arborization in layer 4A made from a single section. Myelinated branches of axon are represented by thick continuous lines. Non-myelinated branches are indicated by thinner continuous lines and boutons are indicated as swellings. Ninety-seven boutons are present in this single field of view from a single section. The stippled drawing of the cortical layer 4A cell represents the visualizable extent (at the light microscope level) of a cell in the axon's terminal field that was filled with HRP reaction-product. Another such cell was located in the adjacent section. *B*, photomicrograph of the HRP-filled cell and part of the axon's terminal field. Note the thick myelinated axon and particularly four of the boutons in the focal plane of which three appear to be contacting the soma-proximal dendrite of the layer 4A cell. *C*, low power electron micrograph (5000 ×) of a thin section taken through the area illustrated in the photomicrograph in *B*. The plane of the section was fortuitous in that the cortical cell containing the HRP reaction-product, the three boutons appearing to contact the cell, the bouton not on the cell and the myelinated axon are all illustrated. Note that the HRP reaction-product is confined to the geniculocortical axon and its processes and the innervated cell. No evidence for HRP leak or uptake into the extracellular space or processes of other cells was observed. The three boutons along the soma-proximal dendrite all made a single synaptic contact with the labelled cortical neurone in

contact. This correlation had been established for the adult in this type of material (Freund *et al.* 1985*a*, *b*), but not for the kitten axons. We thus examined sixty boutons from two kitten axons, as well as an additional eighty-two boutons from one additional adult axon as controls with the electron microscope. From the sample of 142 boutons a total of fifty-four kitten boutons (all from this study) and seventy-five adult boutons (twenty-nine from this study and forty-six from our previous report, Freund *et al.* 1985*a*, *b*) were serially reconstructed. Figure 4 shows an example from a kitten axon of the correlation between the light microscopy and the identification of synaptic boutons at the EM level. This figure also illustrates a phenomenon previously seen in adult material: occasionally (three examples in the kitten axons reported here) HRP reaction-product was found in the soma and proximal dendrites of neurones that received synaptic contacts from the labelled axons. In the example from the kitten shown in Fig. 4*A–D*, three boutons were found to make synaptic contacts with this cell: one synapse was on the soma, two were on a proximal dendrite. This number of synapses between a single afferent and a target cell is in the range previously reported for the adult (Freund *et al.* 1985*b*). As in the equivalent adult material, the ultrastructure of the soma and dendrites are characteristic of smooth cells, which were demonstrated to be GABA-immunoreactive when tested in the adult. The HRP reaction-product is seen only in the postsynaptic neurone. There is no sign of leakage into the extracellular space or into neuronal processes that do not receive synapses from the HRP-filled axon (Fig. 4*C* and *D*). The geniculocortical synapses in both kitten and adult are Gray's type 1, with clear postsynaptic densities.

Most synapses in the kitten were found on dendritic spines (Fig. 5*A* and *B*). When synapses were found on dendritic shafts they tended to be associated with other unlabelled synapses on the same postsynaptic dendrite (Fig. 5*C*). The labelled synapses shown in Fig. 5 were typical of most of the kitten Y-axon boutons. Although the HRP reaction-product was usually very dark, ultrastructural features of the synapse were of sufficiently different electron density that the synaptic vesicles, synaptic membranes and postsynaptic densities were usually discernible. In serial sections, the postsynaptic density was equally likely to appear as a single structure of variable length or initially as a single structure which then split into two separate regions and subsequently rejoined as one density. This pattern suggests an annular synaptic arrangement when fully reconstructed with the spine protruding into a concavity in the bouton. This arrangement was seen both for kittens and adult cat Y-axons. In the adult, single boutons were more likely to make synapses with more than one target (Fig. 6). Occasionally, synapses were also seen on dendritic

---

neighboring serial sections. *D*, higher power (20000×) electron micrograph of most proximal innervating bouton and cortical neurone at a site five sections beyond that illustrated in *C*. Sites of postsynaptic densities at the Gray's type 1 synaptic contact are indicated by arrows. Even though HRP reaction-product was quite dark, vesicles and mitochondria are visible in the bouton and the membrane structure and postsynaptic density are also discernible. The postsynaptic density was observed to become confluent in adjacent serial sections forming a characteristic annular shape and thus comprising a single contact from the bouton.

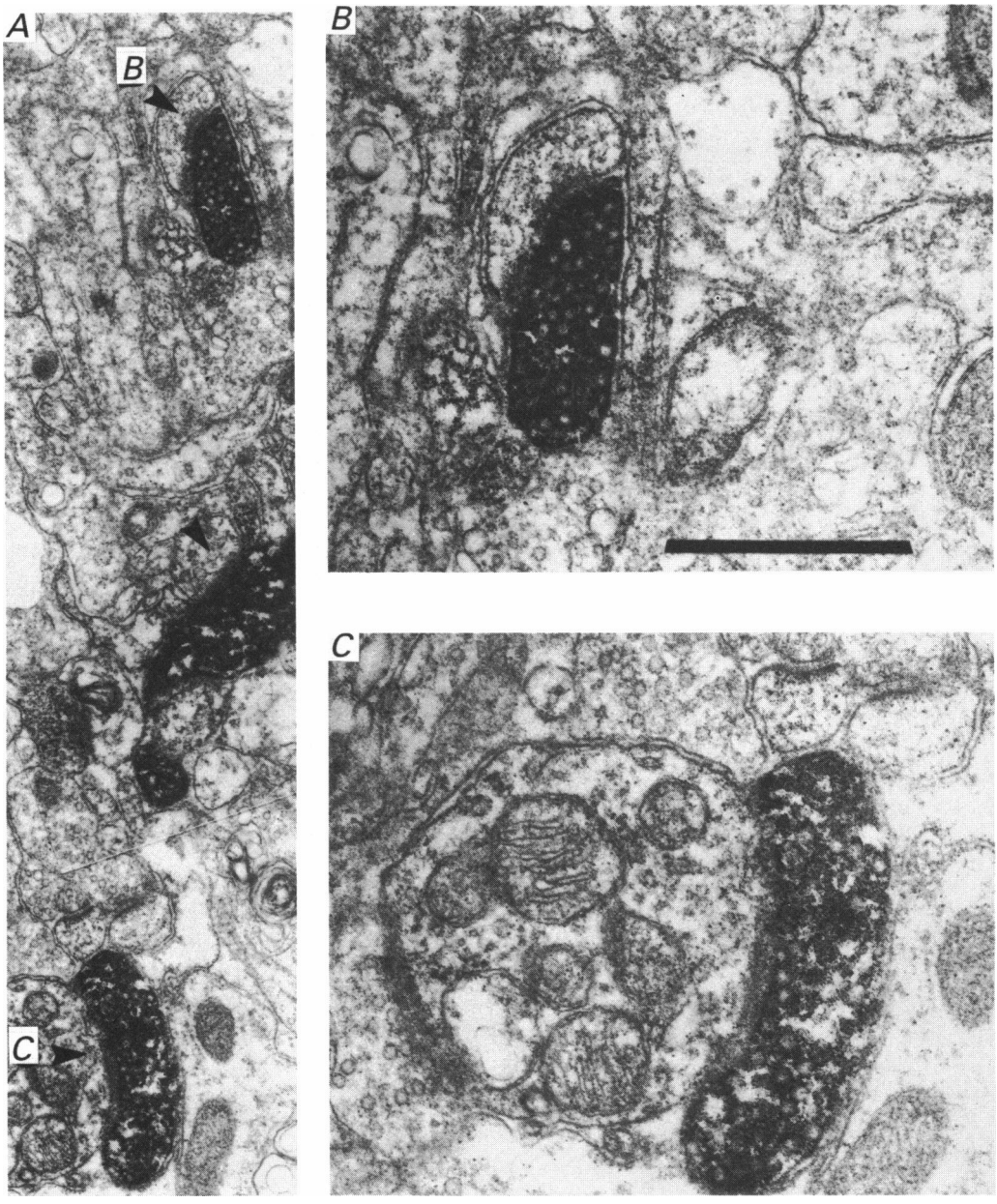

Fig. 5. Representative electron micrographs of HRP-filled synaptic boutons in layer 4A of kitten geniculocortical Y-axons in area 18. *A*, low power EM of several boutons which form single Gray's type 1 synapses with dendritic spines (upper two profiles) and a dendritic shaft (lower profile). All synaptic contacts were verified by tracing the postsynaptic density over serial sections. *B* and *C*, higher power EM of the upper and lower boutons (*B* and *C*) taken from adjacent sections to illustrate synaptic sites. The boutons are closely packed with round vesicles and characteristically innervate a single target as evidenced by serial reconstruction of the contact showing a continuous zone of postsynaptic density. Note that the postsynaptic density is clearly visible although adjacent to the electron-dense HRP reaction-product in the presynaptic terminal. The

shafts (Fig. 6*A* and *E*) and somata. The detailed drawings, light micrographs and low power electron micrographs allowed us to correlate synapses with particular boutons, as shown in Fig. 4. However, for our estimates of the distribution of sites postsynaptic to the boutons and the number of synapses per bouton (Fig. 7 upper and lower, respectively), we used all the synapses we found in a series of sections. The distribution of the target types in kitten and cat were essentially similar: both had spines as their major target type, with the remainder on somata and dendritic shafts (Fig. 7 upper). The kitten boutons had a slight but non-significant preference for spines (89 *vs.* 69%, $P > 0{\cdot}05$, χ-square test).

Of eighty-three boutons that were serially reconstructed, including fifty-four from two kitten axons and twenty-nine from one adult cat axon, together with those from an earlier report on the ultrastructure of over 100 HRP-filled boutons from adult cats (Freund *et al.* 1985*a*, *b*), only four boutons were found to make no synaptic contact. These four boutons were from kitten axons. Moreover, of fifty-nine interbouton axon segments located between the serially reconstructed kitten boutons (as well as between many other boutons which were not fully reconstructed), only two examples of presynaptic elements occurred. These results from our EM studies show that the LM analysis of bouton distribution accurately reflects the actual distribution of the axon's synapses for kitten and adult cat geniculocortical Y-axons. The number of synapses formed by each of the boutons that were fully reconstructed (Fig. 7 lower) was generally one for the kitten axons (82%) and two for the adult axons (57%) with a mean number of synapses per bouton of 1·10 for the kitten and 1·79 for the adult ($P < 0{\cdot}01$, Mann–Whitney U test). Obviously, while we can be reasonably certain that a given bouton seen at light level makes a synapse, we cannot be sure how many synapses it makes.

Light microscopic analysis of kitten and adult axons

Qualitatively, several distinct differences in the axonal arborizations of kitten and adult geniculocortical Y-axons were apparent at the LM level (Fig. 8). The most noticeable differences were in: (1) the size of the boutons (the adult boutons appearing distinctly larger), (2) the apparent density of boutons (appearing higher for kitten axons), (3) the extent of the axon arbor (adult arbors were larger) and (4) the calibre and degree of branching of terminal axon segments (the kitten axon segments appear finer and more branched). Similarities include: (1) the laminar distribution of boutons and (2) both kitten and adult axons form patchy distributions. Some of these differences could be given quantitative expression:

---

bouton illustrated in *B* makes a single Gray's type 1 synaptic contact with a dendritic spine and is very typical of many kitten boutons. The bouton illustrated in *C* makes a single Gray's type 1 synapse upon a dendritic shaft. Note the large diameter and presence of another unlabelled presynaptic terminal forming a Gray's type 2 synapse on the opposite side of the shaft. This arrangement of convergent synaptic input of geniculocortical terminals and profiles from other cells onto dendritic shafts was frequently observed for cases of shaft innervation in the kitten and adult cat. Scale bar 2 μm for panel *A* and 1 μm for panels *B* and *C*.

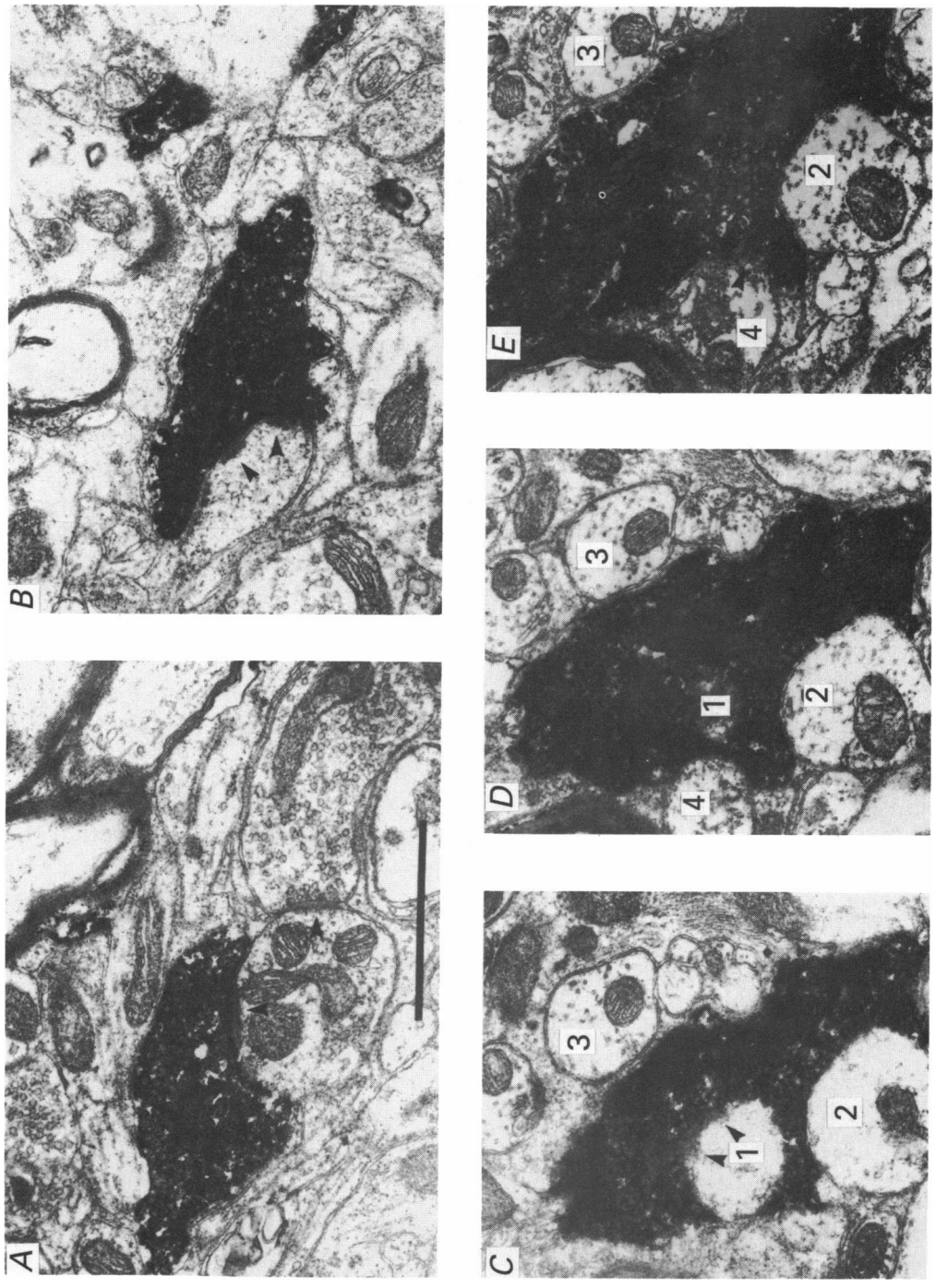

Fig. 6. For legend see facing page.

Bouton size

The adult boutons were larger on average than the kitten boutons. This difference was quantified by measuring the length of a large number of boutons at the LM level at 1200 × magnification. The results plotted in the histogram in Fig. 9 show that the adult boutons are about twice as long as the kitten boutons. These measurements were made along the long axis of the generally ovoid-shaped boutons. However, the widths and lengths of the boutons were sampled on several axons and the same size difference was apparent. The larger size of the adult boutons may relate to the larger number of synapses made per bouton in the adult (Fig. 7). We thus needed to establish the spacing between boutons for the kitten and adult since it was possible that the fewer synapses per bouton in the kitten might be compensated for by having a higher local density than in the adult.

Analyses of bouton spacing and density

Three measures were made using sections from the central portion of the arbors where the most boutons were found. Firstly, we determined the spacing between boutons that lie along the same process, taking into account the three-dimensional nature of the arbors. Figure 10*A* illustrates these interbouton intervals from one of the four central sections of the kitten axon illustrated in Fig. 3*B*. This kitten Y-axon had mean and mode interbouton intervals of 7·5 and 4·5 μm, respectively. This slightly skewed distribution was typical of the kitten Y-axons. Also note that very few intervals of > 12 μm occurred ($< 10\%$). Secondly, we determined the spacing between boutons regardless of whether they were on the same or different branches. The result of this nearest-neighbour analysis of this same axon's boutons is illustrated in Fig. 10*B*. This distribution is heavily skewed and has lower mean (4·5 μm) and mode (3·0 μm) values than for the interbouton interval distribution. Also note that less than 2% of the nearest neighbours are more than 12 μm apart. This indicates that the boutons frequently are in closer proximity to boutons on other branches than adjacent boutons on the same branch. Thirdly, we measured the average density of boutons in three-dimensional space for the central region of the arbor. The total bouton count for the central three sections of this axon yielded an average density of $1{\cdot}42 \times 10^7$ boutons cm^{-3} of cortex.

Fig. 6. Representative electron micrographs of HRP-labelled geniculocortical Y-axon terminals in layer 4A of area 18 from an adult cat. Panels *A* and *B* are high power EMs of two separate boutons that make synaptic contact on a dendritic shaft (*A*) and dendritic spine (*B*), respectively. In each case, the boutons made a single Gray's type 1 synapse with each process. Arrows indicate sites of postsynaptic densities. Note that the dendritic shaft in *A* also receives a synaptic input from another bouton that is unlabelled with HRP and thus from another axon. In all cases, synaptic contacts were followed over multiple serial sections. Scale bar = 1 μm in panels *A–E*. Panels *C–E* are high-power EMs of three of fifty-five serial sections through a single bouton. This bouton made a single Gray's type 1 synapse with each of two dendritic spines and a dendritic shaft. Target number 1 (spine) and number 2 (dendritic shaft) are indicated in the micrographs. Spine number 1 was encapsulated by the bouton. Shaft number 2 was innervated obliquely and the bouton extended a protrusion around the shaft. Note the characteristic large size of the adult Y-axon's bouton. Numbers refer to processes (both those which were and were not innervated by the labelled bouton) to allow reference points for following sections.

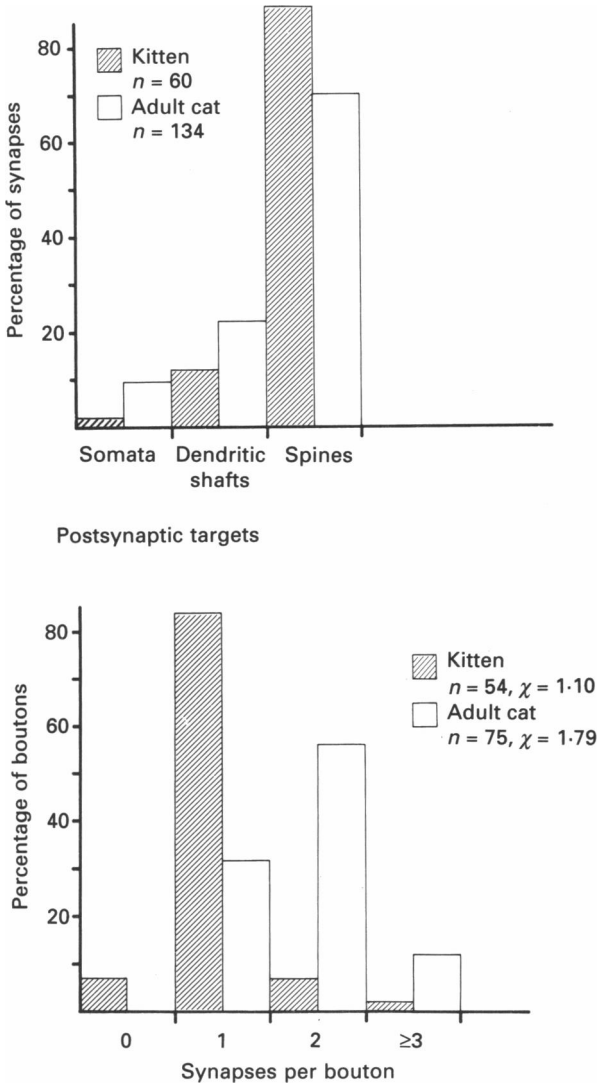

Fig. 7. Summary of distribution of type and number of post synaptic targets for synaptic boutons of kitten and adult geniculocortical Y-axons in layer 4A of area 18. Data are taken from three adult and two kitten axons. Sample sizes for the type and number of synaptic contacts are different as only the boutons for which full serial reconstruction was completed were used for the analysis of number of contacts. Upper histogram, slight but non-significant differences of distributions of synaptic contacts onto spines *vs.* dendritic shafts *vs.* somata were observed for the kitten and adult boutons ($P > 0{\cdot}05$, χ-square test) with a slight preference of the kitten boutons to contact dendritic spines (89 *vs.* 69%). Lower histogram, the distributions of the postsynaptic targets of the kitten and adult boutons are illustrated. These samples differ ($P < 0{\cdot}01$, Mann–Whitney U test) in that most (91%) of the kitten boutons make one or less synapse while most (70%) of the adult boutons contacted two or more postsynaptic targets. The largest number of targets innervated by an adult bouton was four (in two cases, 2·6%). Only one kitten bouton (1·8%) innervated more than two sites (three spines). It is interesting to note that several (four of fifty-four boutons or 7·4%) kitten axon boutons, which were fully serially reconstructed, were not observed to form any synapses. However, it is certainly possible that such a contact might be obscured under particularly adverse conditions of plane of section and geometry of the postsynaptic structure.

The difference in the distribution of boutons in layer 4 between all the kitten and adult cat Y-axons is illustrated in Fig. 11. The upper panel in Fig. 11 demonstrates the relationship between the mean interbouton interval and mean bouton density for the centre of the terminal arborization in layer 4. Each point is the measure for a single axon. An inverse linear relationship exists between these parameters (the

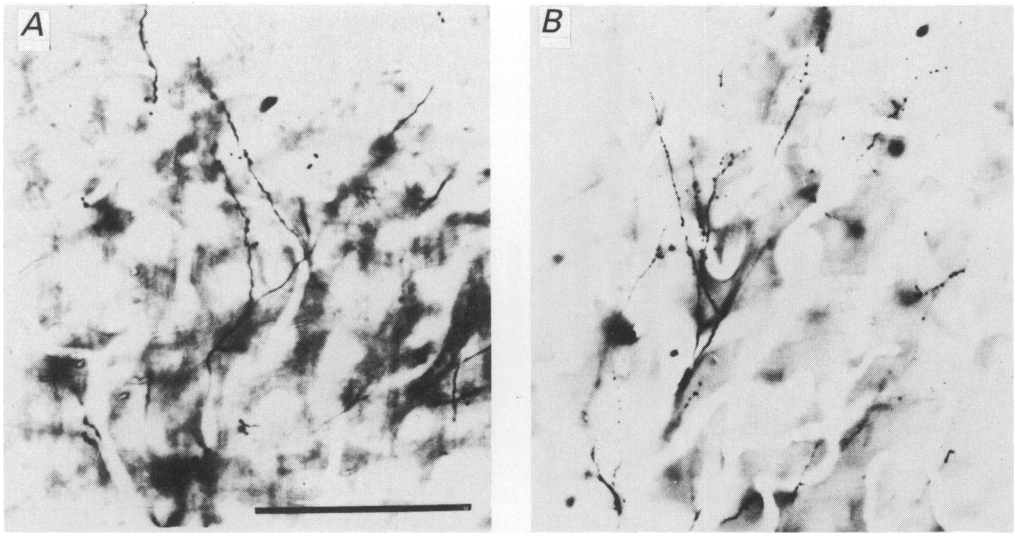

Fig. 8. Photomicrographs of parts of axonal arbor, in layer 4 of adult (*A*) and kitten (*B*) geniculocortical Y-axons taken with a 50 × oil immersion objective. Scale bar = 50 μm. Since the tissue has been osmicated, the contrast between the surrounding regions and clear blood vessels is very high. Note the smaller boutons and higher density of boutons on the kitten axon arbor.

regression line is omitted from the figure for clarity; $y = -4{\cdot}4x + 14{\cdot}6$, correlation coefficient $= -0{\cdot}90$, $P < 0{\cdot}0005$). That is, the overall density of synaptic boutons on a single geniculocortical Y-axon per unit volume of cerebral cortex decreases as the spacing between neighbouring boutons on a given axonal branch increases. The kitten and adult populations of mean interbouton interval and bouton density values are virtually non-overlapping (save for a single adult Y-axon innervating area 18).

The results of the nearest-neighbour analysis (with respect to interbouton interval) are illustrated in the lower panel of Fig. 11. A positive linear correlation between the mean nearest neighbouring bouton and the mean interbouton interval is apparent (the regression line is omitted for clarity; $y = 2{\cdot}7x + 2{\cdot}1$, correlation coefficient $= 0{\cdot}95$, $P < 0{\cdot}0005$). This relationship indicates that axons with closely spaced adjacent boutons on individual branches are also likely to be located close to a bouton on another branch. There is no overlap between the kitten and adult populations for this measure.

Size of axon arbor

The extent of the Y-axons' arborizations within area 18 is slightly smaller for the kitten than the adult axons (Fig. 12). This difference is statistically significant for the

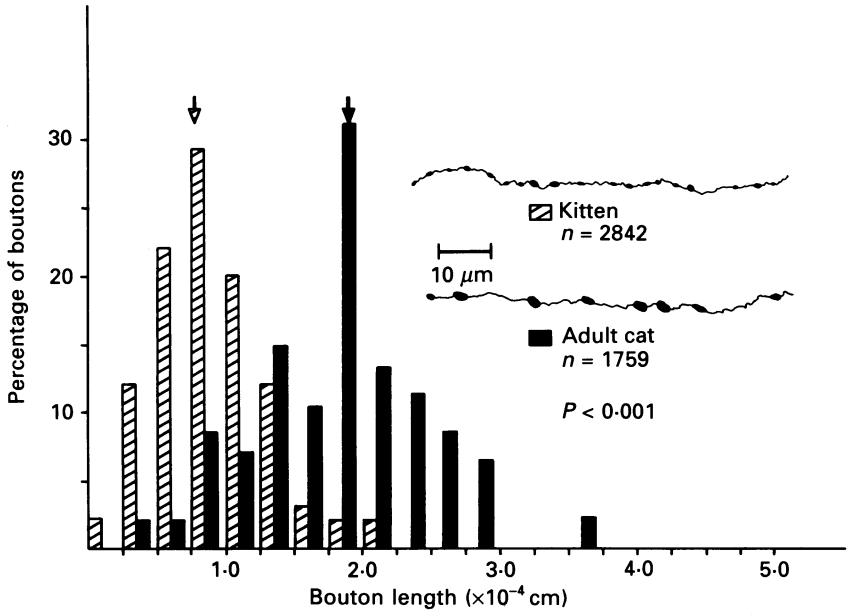

Fig. 9. Frequency distribution histogram of bouton sizes for kitten and adult Y-axons. The bouton sizes are plotted as the length of the longest axis of each bouton as measured with a 100 × oil immersion objective at the light microscope level. Lengths are in bins of 0·25 μm increments which are just at our limit of discrimination with the LM. Boutons were sampled in layer 4A near the centre of the terminal arborization. From 200 to 500 boutons were randomly selected from each axon. The boutons on the kitten Y-axons were significantly smaller than those on the adult Y-axons ($\bar{x}_{\text{kitten}} = 0{\cdot}75$ μm, $\bar{x}_{\text{adult}} = 1{\cdot}75$ μm, $P < 0{\cdot}001$). Inset shows typical example tracings of stretches of boutons from kitten and adult axons.

population of well-filled area 18 Y-axons sampled ($\bar{x}_{\text{kitten}} = 0{\cdot}9$ mm^2, range = 0·4–1·4 mm^2 *vs.* $\bar{x}_{\text{adult}} = 1{\cdot}2$ mm^2, range = 0·7–1·8 mm^2, $P = 0{\cdot}04$, one-tailed Mann–Whitney U test). This increase in the average surface area of $\approx 33\%$ between 4–5 weeks and adult is due to moderate expansion of the extent of the arbors in both the A–P and ML axes from 1·72 to 2·02 mm and from 1·10 to 1·81 mm, respectively. (Note that the surface area measurements are not simply the product of the total A–P and ML extent of the bouton clumps as the ML extent of clump-filled regions of boutons varies considerably between adjacent sections. Thus the area is expressed as the sum of the areas with boutons of each section – see *Methods*.)

DISCUSSION

Four major conclusions can be drawn from this study. First, geniculocortical Y-axons in the 4–5-week-old kitten arborize within area 18 of the visual cortex in a fashion generally similar to those of Y-axons in adult cats and form synapses on the same type of postsynaptic structures in similar proportions. Second, the distribution of synaptic boutons is significantly richer within the centre of the terminal arborizations in layer 4 for the kitten axons than for the adult axons. This higher

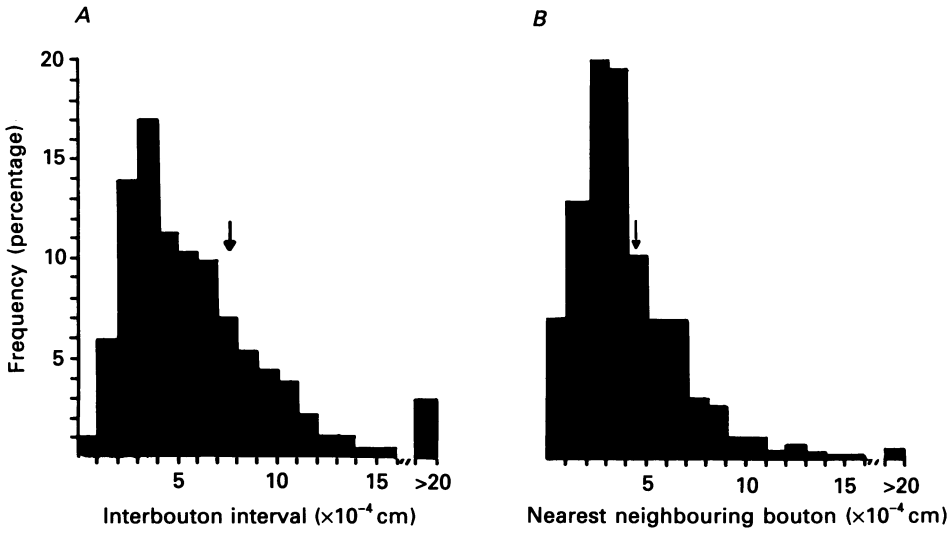

Fig. 10. Example analysis of bouton spacing on layer 4A terminal arborization of kitten geniculocortical Y-axon (same axon illustrated in Fig. 3*B*). *A*, frequency distribution histogram of interbouton intervals for the middle three sections of the central terminal arborization in layer 4A. The vector (in three-dimensional space) from each adjacent bouton on continuous axon branches is calculated by the computer program. $N-1$ intervals (N = the number of boutons on a branch) along a given branch are measured, beginning with the interval between bouton no. 1 and no. 2. The first and last boutons on a branch are identified at the data entry stage so that no measurements between unconnected branches are included in our analysis. The resolution of the measures in three-dimensional space = 0·1 μm. Summarized data are in bins of 1 μm for graphic representation. A total of 1690 interbouton intervals were calculated for the three central sections. The arrow indicates the mean interbouton interval of 7·5 μm. *B*, frequency distribution histogram of nearest neighbour bouton analysis of the same sections analysed in panel *A*. Each bouton serves as the starting point for a single calculation to a nearest neighbour. A vector search occurs to the closest neighbouring bouton (whether it be on the same or a different branch of the same axon's terminal arborization) in three-dimensional space and this value is stored. The outlying boutons in the *Z*-axis on the end sections are omitted from the analysis if the distance to the outer surface of the section was less than the distance to any neighouring bouton within the section. The mean nearest neighbour value = 4·5 μm as indicated by the arrow.

bouton density on individual kitten axons occurs both along individual axon branches (interbouton interval) and between branches (nearest-neighbour distribution and bouton density per unit volume of cerebral cortex). Third, the surface area of layer 4 innervated by kitten Y-axons is less than that of adult Y-axons. The increase in surface area innervated by an individual axon during development is primarily due to the expansion in the mediolateral axis. Fourth, the boutons on kitten Y-axons are significantly smaller and make fewer synapses on average than those of adult Y-axons. Some of these differences are summarized schematically in Fig. 13.

Development of geniculocortical innervation – expansion or retraction?

Evidence from a variety of sites in the nervous system supports the hypothesis that an initial overproduction of axon branches, synapses and/or neurones is

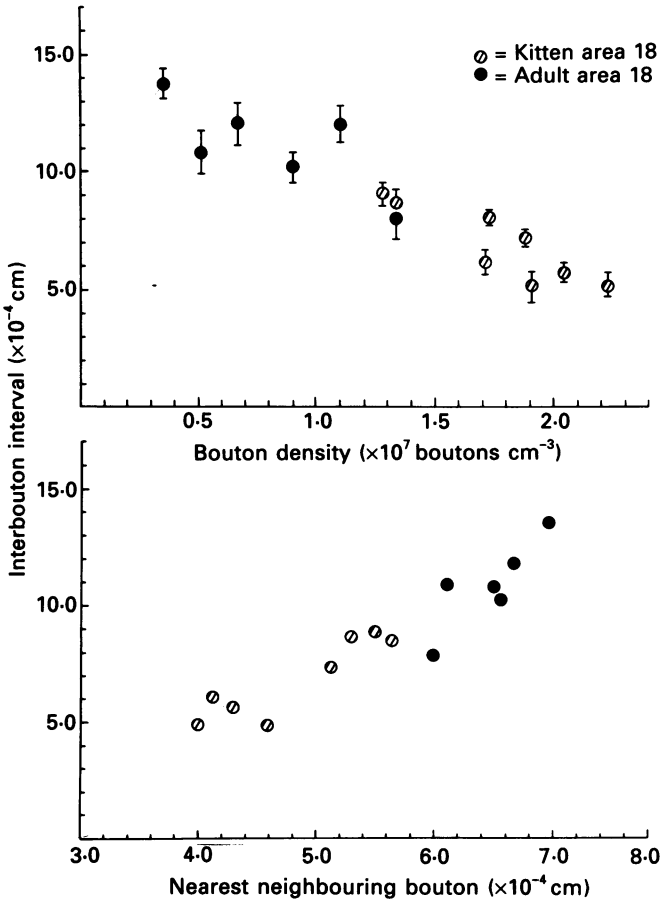

Fig. 11. Scatter diagram of relationship between mean interbouton interval (IBI) *vs.* bouton density (upper panel) and nearest neighbouring bouton (lower panel) for individual kitten and adult geniculocortical Y-axons. Upper panel, the mean IBI values were computed for the central field of each axon's terminal arborization in cortical layer 4 as described in Fig. 8. These values were plotted ± S.E.M. as a function of the average bouton density (described in Methods). These parameters are well correlated (see text) such that both kitten and adult Y-axons with greater bouton densities in three-dimensional space also have shorter interbouton intervals. The grand mean of bouton density is significantly greater for the kitten axons than the adult axons ($\bar{x}_{\text{kitten}} = 1{\cdot}7 \times 10^7$ boutons cm^{-3} *vs.* $\bar{x}_{\text{adult}} = 0{\cdot}8 \times 10^7$ boutons cm^{-3}, $P < 0{\cdot}001$) and the grand mean of the interbouton intervals is significantly less for the kitten than the adult axons ($\bar{x}_{\text{kitten}} = 6{\cdot}6$ μm, $\bar{x}_{\text{adult}} = 11{\cdot}2$ μm, $P < 0{\cdot}001$).

followed by a loss of a portion of these during development (neuromuscular junction, Redfern, 1970; Brown, Jansen & Van Essen, 1976; see Van Essen (1982) for a review; cerebellum, Crepel, Marciani & Delheye-Bouchard, 1976; autonomic ganglia, Lichtman, 1977; Lichtman & Purves, 1980; retinal projections, Rakic & Riley, 1983; Shatz, 1983; Sur *et al.* 1984; visual cortex, Innocenti *et al.* 1977; Innocenti, 1981; Dehay, Bullier & Kennedy, 1984; see Purves & Lichtman, 1984 for a review for all of these sites). Our data directly demonstrate that in the 4–5-week-old kitten, the

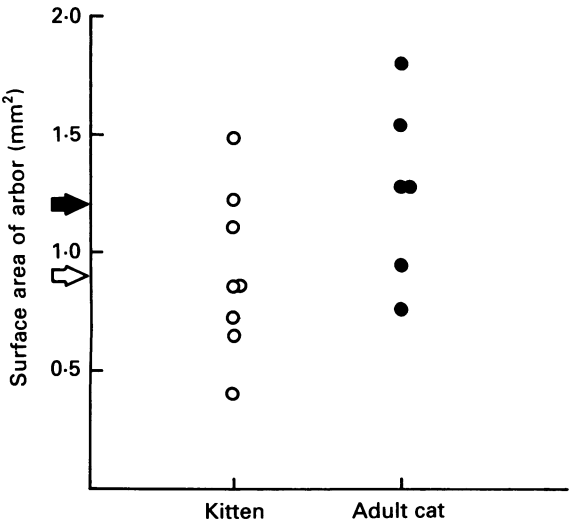

Fig. 12. Distribution plot of size of surface areas of terminal arborizations of kitten (○) and adult cats (●) geniculocortical Y-axons projecting to area 18. Arrows indicate mean value ($\bar{x} = 0{\cdot}9$ mm² in kitten and $\bar{x} = 1{\cdot}2$ mm² in the adults). These values differ significantly between the two groups ($P = 0{\cdot}04$, Mann–Whitney U test).

geniculocortical Y-axon arborizations in area 18 are smaller than those in the adult. These data do not support the hypothesis of a retraction of an initially expanded projection but suggest instead that this thalamocortical innervation develops by a moderate expansion of the arborizations. Concomitantly, there is a reduction in a single axon's bouton density at the centre of each arborization. A similar postnatal expansion in the size of axonal arborizations has been observed for retinogeniculate Y-axons in kittens of the same age (Sur *et al.* 1984; Friedlander *et al.* 1985). This expansion may contribute to the decrease in average bouton density (per axon within a unit volume at the centre of the arborization) during development. It should be noted that this expansion of the arbors is in real terms. It is possible that the surface area of area 18 is also expanding at a similar (or greater) rate during this same period of development. If this were so, the actual expansion of the axon arborization could be offset in functional terms with respect to visuotopic spread.

The increased spacing of boutons (both within and between axon branches) may also result from additional elimination of boutons, elongation of the interbouton axon segments, separation of neighbouring branches and/or a fusion of adjacent boutons on a single branch. We cannot yet discriminate between these mechanisms. However, our data showing that the adult boutons are larger, their spacing greater and that they make more synapses on average than the kitten Y-axon boutons lend credence to the hypothesis that adjacent boutons fuse, simultaneously reducing the bouton number and increasing the synapses per bouton. The change in the number of geniculocortical synapses/cortical cell ratio (see below) is only about 10%. It thus seems unlikely that the massive loss of axospinous synapses in the cortex during development (Winfield, 1981) is due specifically to a loss of geniculocortical synapses during the process of column formation in development. In fact the opposite trend

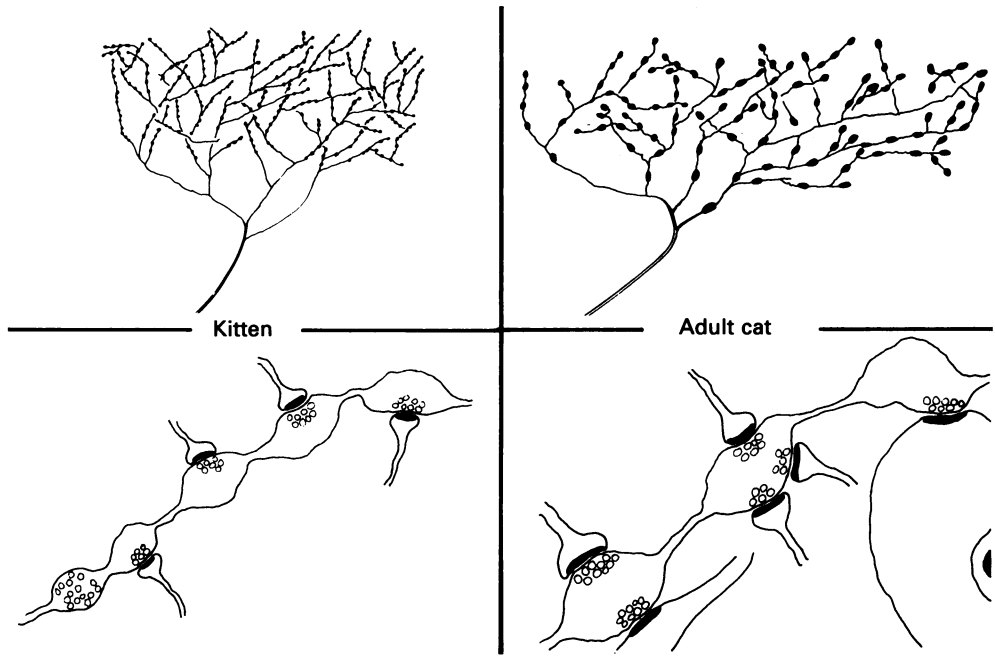

Fig. 13. Summary diagram of difference in structure of terminal arborizations of kitten *vs.* adult geniculocortical Y-axons projecting to cortical area 18 as observed at the light and electron microscopic levels. Note the smaller extent of the kitten arbors, smaller boutons, shorter interbouton distances on a given axonal branch and higher density of boutons with respect to neighbouring branches. The ultrastructural differences represented include smaller and more closely packed boutons in the kitten that generally only make a single synaptic contact, usually on a dendritic spine, *vs.* larger more widely spaced boutons in the adult that favour multiple synaptic contacts with slightly less preference for dendritic spines.

might well have been predicted from the observation that in young kittens the responses of cortical neurones are sluggish and easily fatigued (Hubel & Wiesel, 1963). The improvement in responsiveness seen through development is probably due to many factors, of which functional maturation of the synapse is only one.

Development of ocular dominance columns – relation to previous studies

It is of interest to compare our results from area 18 to previous studies on the development of area 17 and the elaboration of ocular dominance columns in visual cortex. The anatomical development of the geniculocortical innervation in the kitten has been evaluated primarily by anterograde tracer studies. Kato, Kawaguchi, Yamamoto, Samejima & Miyata (1983) described an increase in the density of the geniculocortical innervation in layer 4 of kitten visual cortex between 1 and 4–6 postnatal weeks as visualized by anterograde bulk HRP transport. These results were primarily obtained from area 17 but the authors state, 'The case is similar in area 18.' Since this study did not include an adult control group, it is not apparent whether the geniculocortical innervation density dropped after peaking at 4–6

weeks. However, the data support our finding that the bouton density of single geniculocortical Y-axons is higher at 4–5 weeks of age than in the adult cat. The results of Cragg (1975) offer further support for our finding as he reported a peak total synaptic density at ≈ 5 weeks in kitten area 17 that declined by ≈ 40% in the adult cat.

LeVay *et al.* (1978) reported that ocular dominance columns in kitten area 17 (as demonstrated by autoradiography of transneuronally transported [^{3}H]proline after single eye injections) are less distinct than in adult cat. While the finding was most apparent in very young kittens (8–22 days), immature column formation was also seen in a 33-day-old kitten, the age group that we studied (LeVay *et al.* 1978; column segregation index of 0·25 *vs.* 0·75 for the visual cortex ipsilateral to the eye injection). It has been speculated that the progressive column segregation during development results from gaps formed by selective pruning of hypertrophied homogeneous arborizations of single geniculocortical axons (LeVay & Stryker, 1979; Shatz & Luskin, 1986). Our results on the surface area of geniculocortical Y-axon arborizations contrast with this conclusion, showing a modest (≈ 33%) but significant ($P = 0{\cdot}04$) increase in the extent of arborizations. There are several possible explanations for the apparent difference in the results on ocular dominance column formation in area 17 and our results on the development of individual geniculocortical axons innervating area 18.

First, there may be fundamental differences in the development of geniculocortical innervation between these two cortical areas. As already described (see Introduction), the layer 4 cortical innervation by the LGN_d differs for these areas by virtue of area 18 only receiving a Y-cell input. Thus, the opportunity for X/Y competitive interactions in area 17 in addition to binocular competition may add another level of complexity. Physiologically, the percentage of binocularly activated neurones in area 17 decreases from about 79 to 60% from about 2 weeks of age to adult (LeVay *et al.* 1978). Similarly, Albus & Wolf (1984) report about 74% binocularly activated neurones (mostly from area 17 although they include some area 18 neurones in their study) in kittens of similar age. However, the results from studies confined exclusively to area 18 suggest a different developmental process. Milleret *et al.* (1988) report that the percentage of binocularly activated cortical neurones *increases* dramatically from 33 to 72% between 2 and 4 weeks of age with a further increase to 76% at adult. Blakemore & Price (1987) find very little change in binocularly activated cortical cells during the postnatal development of area 18 (100 *vs.* 95% in 1-week-old kittens *vs.* adult cats). Although the quantitative expression of the changing fraction of binocular cells varies somewhat between laboratories, it seems clear that the physiological development of binocularity in area 18 does not mirror that in area 17. The physiological evidence in area 18 does not support the notion of a reduction in binocular mixing during development as has been described for area 17. These results are in agreement with our anatomical findings of a modest increase (*vs.* retraction) in the extent of geniculocortical axon arborizations in area 18, since this may be expected to result in increasing opportunity for binocular mixing of excitatory geniculocortical drive during development. It is also possible that the physiological development of binocularity reflects maturation of intracortical circuitry.

Second, the mechanisms of geniculocortical development in areas 17 and 18 may be similar. To date, no comparable direct data on the development of physiologically *identified* geniculocortical axons innervating area 17 are available for comparison to our area 18 projecting axons. A re-ordering of the terminal arborizations of individual axons with respect to its neighbours in a column could account for the different conclusions reached from the area 17 autoradiography data and the area 18 single axon data. The obscure nature of the columns viewed autoradiographically in kitten area 17 might result from less precise overlap of arbors from neighbouring layer A or layer A_1 LGN_d Y-cell axons. During postnatal development, the individual arbors could expand (as they do in area 18) into overlapping zones while simultaneously reducing extraneous branches and boutons that impinge on neighbouring columns. In order to test this hypothesis, individual kitten and adult cat axonal arborizations must be stained in conjunction with labelling of the entire ocular dominance columns.

Third, the difference in the results from area 17 and area 18 may be of a longitudinal nature. This is, the postnatal development of geniculocortical axon arborizations may proceed by different strategies at various stages of development such that the arborizations expand beyond adult territories after reaching the innervation site (Shatz & Luskin, 1986). This period may be followed by a time characterized by retraction and increased specificity of connections and then by additional moderate growth. In order to evaluate this hypothesis it will be necessary to collect data on axons at a variety of ages using the methods employed in our study. However, it is worth noting that the results of LeVay *et al.* (1978) in area 17 indicate that the ocular dominance columns are qualitatively similar in their lack of definition at 33 days as well as at 2 weeks of age, although quantitatively less so.

The coverage of cortex by Y-axons

The reduction in the bouton density of individual geniculocortical Y-axons during development has an important functional consequence for average geniculocortical convergence and cortical coverage factors. The mean bouton density per Y-axon decreases between 4–5 postnatal weeks and adult. Cragg (1975, his Fig. 7) reported that during this same period, the density of neurones in visual cortex does not change significantly. Therefore, the decrease in Y-axon bouton density reflects a true decrease in average geniculocortical innervation density and not simply a concurrent expansion of the axonal arborizations with cortical growth. By combining our analyses with Cragg's values for visual cortex neurone density, we conclude that on average, each adult geniculocortical Y-axon in area 18 provides approximately one synapse for every 2·9 cortical neurones within the central region of its terminal arborization. A similar calculation for the kitten yields one synapse per 2·6 cortical neurones. Moreover, the change in the coverage factor (the number of geniculocortical axons that contribute to the innervation of a unit volume of cortex) can be similarly calculated. This calculation utilizes Cragg's (1975) values for average total synapse density in kitten and adult cat area 17 and estimated percentage of these synapses that are geniculocortical (we split the value of the estimates of Garey & Powell (1971) and LeVay & Gilbert (1976)). This calculation yields values of 3267 and 3777 for the kitten and adult cat area 18 Y-axons, respectively; i.e. at every point in layer 4 of

area 18 the neurones could *potentially* be contacted by 3267 or 3777 LGN_d axons in the kitten and adult cat, respectively. As might be expected from this, small extracellular HRP injections in adult cat area 18 label cells over a considerable extent of the LGN (Geisert, 1985). A similar calculation for adult geniculocortical X-axons in area 17 (Freud *et al.* 1985*b*) estimated a coverage factor of 880. Thus the spatial overlap of area 18 Y-axons is 4–5 times greater than for area 17 X-axons in adult cats. This conclusion is consistent with the greater reported divergence of Y- *vs.* X-geniculocortical axons in adult cat (Humphrey *et al.* 1985*a*, *b*) and our suggestion of serial expansion of the entire Y pathway from retina to visual cortex (Friedlander *et al.* 1981; Freund *et al.* 1985*a*; Sherman, 1985). Moreover, the results of our calculations suggest that a 15% increase in potential cortical coverage by Y-axons in area 18 occurs from 4–5 weeks postnatal onward. This is consistent with the increase in extent of individual Y-axon arborizations during this period.

Development of the Y-cell pathway

Considerably fewer Y-cells are recorded in the A layers of the LGN_d at 4–5 postnatal weeks than in the adult cat (17 *vs.* 33%, Friedlander *et al.* 1981; Friedlander & Stanford, 1984; Tootle & Friedlander, 1986, 1989; Friedlander & Tootle, 1989). However, the cells that already exhibit the physiological property of non-linear spatial summation at 4–5 weeks are morphologically very similar (but smaller in soma size and dendritic extent) to their adult counterparts (Friedlander, 1982, 1984; Tootle & Friedlander, 1986). We have also observed a similar morphological maturity for physiologically identifiable Y-cells in the LGN_d magnocellular C layer and medial interlaminar nucleus (MIN) in kittens of this same age (J. S. Tootle and M. J. Friedlander, unpublished observations). Therefore, reduction in bouton density, increase in extent of the terminal arborizations and increase in bouton size for the axons' aborization parallel the increase in somatic and dendritic extent of Y-cells. Moreover, the extent of the retinal innervation of the LGN_d by Y ganglion cells also increases during this same period both in relative (Friedlander *et al.* 1985) and absolute (Sur *et al.* 1984; Friedlander *et al.* 1985) terms. Therefore, from 4–5 weeks, the retino-geniculo-cortical Y system expands at all levels (expansion of arborizations of individual retinal ganglion cell axons, increase in soma and dendritic extent of LGN_d Y-cells and expansion of the extent of the terminal arborization of geniculocortical axons). These growth processes are paralleled by a reduction in geniculocortical axon bouton density and possibly a reduction in dendritic spine density on LGN_d Y-cells (Friedlander, 1982; Mason, 1984; Tootle & Friedlander, 1986) and on cortical neurones (Boothe, Greenough, Lund & Wrege, 1979).

Relation of the critical period

Considerable anatomical and physiological evidence supports the particular susceptibility of the Y-cell system to abnormal binocular vision during the critical period (see Sherman & Spear (1982) for a review). The construct of binocular competition (Wiesel & Hubel, 1963; Hubel & Wiesel, 1970; Hubel *et al.* 1977) has served as a useful model for explaining these effects. The specific structural changes in individual geniculocortical Y-axons during normal development may underlie the

sensitivity to unequal binocular vision at this age. The boutons become less densely packed and the terminal arborizations expand their territory during normal postnatal development. Unequal binocular input (e.g. monocular visual deprivation) may affect these processes directly by affecting their rates and/or their duration. Thus, the degree of functional convergent drive to single cortical neurones from multiple boutons from individual thalamic afferents (see Fig. 4) and from multiple thalamic afferents could be altered. It will be of interest to analyse the structure and ultrastructure of similarly stained and physiologically identified geniculocortical axons in animals reared with monocular deprivation.

This research was supported by NIH grant EY-05116, the Wellcome Trust and the MRC (UK), NATO Grant 86/0575, the Alfred P. Sloan Foundation and the UAB Neurobiology Research Center Cell Reconstruction Facility. We thank Mr John Anderson and Ms Judith Rodda for their excellent technical work, Ms Jill Gemmill and Mr Kevin Ramer for computer processing and Ms Vinessa Alones for her excellent electron microscopy skills. We thank Dr James R. Wilson and Ms Pat Fancher who assisted with some of the preliminary analysis of the kitten EM materials and Dr John S. Tootle for help with some of the preliminary experiments in this project. We also thank Ms Evelyn Shearer for her excellent word processing skills.

REFERENCES

ADAMS, J. C. (1981). Heavy metal intensification of DAB based HRP reaction product. *Journal of Histochemistry and Cytochemistry* **29**, 775.

ALBUS, K. & WOLF, W. (1984). Early postnatal development of neuronal function in the kitten's visual cortex: a laminar analysis. *Journal of Physiology* **348**, 153–185.

BARLOW, H. B. & PETTIGREW, J. D. (1971). Lack of specificity of neurones in the visual cortex of young kittens. *Journal of Physiology* **218**, 98–100*P*.

BLAKEMORE, C. & PRICE, D. J. (1987). The organization and postnatal development of area 18 of the cat's visual cortex. *Journal of Physiology* **384**, 263–292.

BLAKEMORE, C. & VAN SLUYTERS, R. C. (1975). Innate and environmental factors in the development of kitten visual cortex. *Journal of Physiology* **248**, 663–716.

BONDS, A. B. (1979). Development of orientation tuning in visual cortex of kittens. In *Developmental Neurobiology of Vision*, ed. FREEMAN, R. D., pp. 31–41. New York: Plenum Press.

BOOTHE, R. G., GREENOUGH, W. T., LUND, J. S. & WREGE, K. (1979). A quantitative investigation of spine and dendrite development of neurones in visual cortex (area 17) of *Macaca nemestrina* monkeys. *Journal of Comparative Neurology* **186**, 473–490.

BRAASTADT, B. O. & HEGGELUND, P. (1985). Development of spatial receptive-field organization and orientation selectivity in kitten striate cortex. *Journal of Neurophysiology* **53**, 1158–1178.

BROWN, M. C., JANSEN, J. K. S. & VAN ESSEN, D. (1976). Polyneuronal innervation of skeletal muscle in newborn rats and its elimination during maturation. *Journal of Physiology* **261**, 387–422.

BUISSERET, P. & IMBERT, M. (1976). Visual cortical cells: their developmental properties in normal and dark reared kittens. *Journal of Physiology* **255**, 511–525.

CRAGG, B. G. (1975). The development of synapses in the visual system of the cat. *Journal of Comparative Neurology* **160**, 147–166.

CREPEL, F., MARCIANI, J. & DELHEYE-BOUCHARD, N. (1976). Evidence for a multiple innervation of Purkinje cells by climbing fibres in the immature rat cerebellum. *Journal of Neurobiology* **7**, 567–578.

DEHAY, C., BULLIER, J. & KENNEDY, H. (1984). Transient projections from the frontoparietal and temporal cortex to Areas 17, 18 and 19 in the kitten. *Experimental Brain Research* **57**, 208–212.

DERRINGTON, A. M. & FUCHS, A. F. (1981). The development of spatial-frequency selectivity in kitten striate cortex. *Journal of Physiology* **316**, 1–10.

FERSTER, D. (1987). Segregation of X and Y afferents into areas 17 and 18 of cat visual cortex. *Society for Neuroscience Abstracts* **13**, 1449.

FREGNAC, Y. & IMBERT, M. (1984). Development of neuronal selectivity in primary visual cortex of cat. *Physiological Reviews* **64**, 325–434.

FREUND, T., MARTIN, K. A. C., SOMOGYI, P. & WHITTERIDGE, D. (1985*b*). Innervation of cat visual areas 17 and 18 by physiologically identified X- and Y-type thalamic afferents. II. Identification of postsynaptic targets by GABA immunocytochemistry and Golgi impregnation. *Journal of Comparative Neurology* **242**, 275–291.

FREUND, T. F., MARTIN, K. A. C. & WHITTERIDGE, D. (1985*a*). Innervation of cat visual areas 17 and 18 by physiologically identified X- and Y-type thalamic afferents. I. Arborization patterns and quantitative distribution of postsynaptic elements. *Journal of Comparative Neurology* **242**, 263–274.

FRIEDLANDER, M. J. (1982). Structure of physiologically classified neurones in the kitten dorsal lateral geniculate nucleus. *Nature* **200**, 180–183.

FRIEDLANDER, M. J. (1984). The postnatal development of the kitten dorsal lateral geniculate nucleus. In *Development of Visual Pathways in Mammals*, ed. STONE, J., DREHER, B. & RAPPAPORT, D., pp. 155–173. New York: Alan R. Liss Press.

FRIEDLANDER, M. J. (1988). The dynamic and distributive properties of the dorsal lateral geniculate nucleus. *Proceedings of the Australian Physiological and Pharmacological Society* **19**, 44–55.

FRIEDLANDER, M. J., LIN, C.-S., STANFORD, L. R. & SHERMAN, S. M. (1981). Morphology of functionally identified neurons in the dorsal lateral geniculate nucleus of cat. *Journal of Neurophysiology* **46**, 80–129.

FRIEDLANDER, M. J., MARTIN, K. A. C. & TOOTLE, J. S. (1984). Postnatal development of geniculocortical Y-axon terminal arborizations in area 18 of the cat. *Society for Neuroscience Abstracts* **10**, part 2, 1077.

FRIEDLANDER, M. J., MARTIN, K. A. C., & VAHLE-HINZ, C. (1985). The structure of the terminal arborizations of physiologically identified retinal ganglion cell Y-axons in the kitten. *Journal of Physiology* **359**, 293–313.

FRIEDLANDER, M. J. & STANFORD, L. R. (1984). Effects of monocular deprivation on the distribution of cell types in the l.g.n.: A sampling study with fine-tipped micropipettes. *Experimental Brain Research* **53**, 451–461.

FRIEDLANDER, M. J., STANFORD, L. R. & SHERMAN, S. M. (1982). Effects of monocular deprivation on the structure/function relationship of individual neurons in the cat's lateral geniculate nucleus. *Journal of Neuroscience* **2**, 321–330.

FRIEDLANDER, M. J. & TOOTLE, J. S. (1989). Postnatal anatomical and physiological development of the visual system. In *Development of Sensory Systems in Mammals*, ed. COLEMAN, J. R. New York: John Wiley and Sons (in the Press).

FRIEDLANDER, M. J., WILSON, J. R., MARTIN, K. A. C., FANCHER, P. & ALONES, V. (1986). Postnatal development of the Y-cell geniculocortical synapse in kitten area 18. *Investigative Opthalmology and Visual Science* **27**, suppl., 224.

GAREY, L. J. & POWELL, T. P. S. (1971). An experimental study of the termination of the lateral geniculo-cortical pathway in the cat and monkey. *Proceedings of the Royal Society* B **179**, 41–63.

GEISERT, E. E. (1985). The projection of the lateral geniculate nucleus to area 18. *Journal of Comparative Neurology* **238**, 101–106.

GILBERT, C. D. & WIESEL, T. N. (1979). Morphology and intracortical projections of functionally characterized neurones in the cat visual cortex. *Nature* **280**, 120–125.

HANKER, J. S., YATES, P. E., METZ, C. B. & RUSTIONI, A. (1977). A new specific, sensitive and non-carcinogenic reagent for the demonstration of horseradish peroxidase. *Histochemistry Journal* **9**, 789–792.

HENDERSON, F. (1982). An anatomical investigation of projections from lateral geniculate nucleus to visual cortical areas 17 and 18 in newborn kittens. *Experimental Brain Research* **46**, 177–185.

HOCHSTEIN, S. & SHAPLEY, R. M. (1976*a*). Quantitative analysis of retinal ganglion cell classification. *Journal of Physiology* **262**, 237–264.

HOCHSTEIN, S. & SHAPLEY, R. M. (1976*b*). Linear and nonlinear subunits in Y cat retinal ganglion cells. *Journal of Physiology* **262**, 265–284.

HUBEL, D. H. & WIESEL, T. N. (1963). Receptive fields of cells in striate cortex of very young, visually inexperienced kittens. *Journal of Neurophysiology* **26**, 994–1002.

HUBEL, D. H. & WIESEL, T. N. (1965). Receptive fields and functional architecture in 2 non-striate visual areas (18 & 19) of the cat. *Journal of Neurophysiology* **28**, 229–289.

HUBEL, D. H. & WIESEL, T. N. (1970). The period of susceptibility to the physiological effects of unilateral eye closure in kittens. *Journal of Physiology* **160**, 106–154.

HUBEL, D. H., WIESEL, T. N. & LEVAY, S. (1977). Plasticity of ocular dominance columns in monkey striate cortex. *Philosophical Transactions of the Royal Society* B **278**, 377–409.

HUMPHREY, A., SUR, M., UHLRICH, D. & SHERMAN, S. M. (1985*a*). Projection patterns of individual X- and Y-cell axons from the lateral geniculate nucleus to cortical area 17 in the cat. *Journal of Comparative Neurology* **233**, 159–189.

HUMPHREY, A., SUR, M., UHLRICH, D. & SHERMAN, S. M. (1985*b*). Termination patterns of individual X- and Y-cell axons in the visual cortex of the cat: Projections to area 18, to the 17/18 border region, and to both areas 17 and 18. *Journal of Comparative Neurology* **233**, 190–212.

INNOCENTI, G. M. (1981). Growth and reshaping of axons in the establishment of visual callosal connections. *Science* **212**, 824–827.

INNOCENTI, G. M., FIORE, L. & CEMONITI, R. (1977). Exuberant projections into the corpus callosum from the visual cortex of newborn cats. *Neuroscience Letters* **4**, 437–442.

KATO, N., KAWAGUCHI, S., YAMAMOTO, T., SAMEJIMA, A. & MIYATA, H. (1983). Postnatal development of the geniculocortical projection in the cat: Electrophysiological and morphological studies. *Experimental Brain Research* **51**, 65–72.

KOPPEL, H. & INNOCENTI, G. M. (1983). Is there a genuine exuberancy of callosal projections during development? A quantitative electron microscopical study in the cat. *Neuroscience Letters* **41**, 33–40.

LEVAY, S. & GILBERT, C. D. (1976). Laminar patterns of geniculocortical projections in the cat. *Brain Research* **113**, 1–19.

LEVAY, S. & STRYKER, M. P. (1979). The development of ocular dominance columns in the cat. In *Aspects of Developmental Neurobiology* (Society for Neuroscience Symposium), ed. FERENDELLI, J. A., pp. 83–98. Bethesda, MD, USA: Society for Neuroscience.

LEVAY, S., STRYKER, M. P. & SHATZ, C. J. (1978). Ocular dominance columns and their development in layer IV of the cat's visual cortex: A quantitative study. *Journal of Comparative Neurology* **179**, 223–244.

LICHTMAN, J. W. (1977). The reorganization of synaptic connexions in the rat submandibular ganglion during post-natal development. *Journal of Physiology* **273**, 155–177.

LICHTMAN, J. W. & PURVES, D. (1980). The elimination of redundant preganglionic innervation to hamster sympathetic ganglion cells in early post-natal life. *Journal of Physiology* **301**, 213–228.

LUND, J. S., HENRY, G. H., MACQUEEN, C. L. & HARVEY, A. R. (1979). Anatomical organization of the primary visual cortex (area 17) of the cat. A comparison with area 17 of the Macaque monkey. *Journal of Comparative Neurology* **184**, 599–618.

MANGEL, S. C., WILSON, J. R. & SHERMAN, S. M. (1983). Development of neuronal response properties in the cat dorsal lateral geniculate nucleus during monocular deprivation. *Journal of Neurophysiology* **50**, 240–264.

MASON, C. A. (1984). Postnatal maturation of cat dorsal lateral geniculate nucleus. *Journal of Comparative Neurology* **219**, 458–469.

MILLERET, C., GARY-BOBO, E. & BUISSERET, P. (1988). Comparative development of cell properties in cortical area 18 of normal and dark-reared kittens. *Experimental Brain Research* **71**, 8–20.

O'LEARY, J. L. (1941). Structure of the area striata of the cat. *Journal of Comparative Neurology* **75**, 131–161.

PRICE, D. J. & BLAKEMORE, C. (1985). The postnatal development of the association projection from visual cortical area 17 to area 18 in the cat. *Journal of Neuroscience* **5**, 2443–2452.

PURVES, D. & LICHTMAN, J. W. (1984). *Principles of Neural Development*. Sunderland, MA, USA: Sinauer Associates.

RAKIC, P. & RILEY, K. P. (1983). Overproduction and elimination of retinal axons in the fetal rhesus monkey. *Science* **219**, 1441–1443.

REDFERN, P. A. (1970). Neuromuscular transmission in new-born rats. *Journal of Physiology* **209**, 701–709.

SHATZ, C. J. (1983). The prenatal development of the cat's retinogeniculate pathway. *Journal of Neuroscience* **3**, 482–499.

SHATZ, C. J. & LUSKIN, M. B. (1986). The relationship between the geniculocortical afferents and their cortical target cells during development of the cat's primary visual cortex. *Journal of Neuroscience* **6**, 3655–3668.

SHERMAN, S. M. (1985). Functional organization of the W-, X- and Y-cell pathways in the cat: a review and hypothesis. *Proceedings of Physiological Psychology* **11**, 233–315.

SHERMAN, S. M., HOFFMAN, K.-P. & STONE, J. (1972). Loss of a specific cell type from the dorsal lateral geniculate nucleus in visually deprived cats. *Journal of Neurophysiology* **35**, 532–541.

SHERMAN, S. M. & SPEAR, P. D. (1982). The organization of visual pathways in normal and visually deprived cats. *Physiological Reviews* **62**, 738–855.

STONE, J. (1983). Parallel processing in the visual system – the classification of retinal ganglion cells and its impact on the neurobiology of vision. In *Perspectives of Vision Research*, ed. BLAKEMORE, C. New York: Plenum Press.

STONE, J. & DREHER, B. (1973). Projections of X- and Y-cells of the cat's lateral geniculate nucleus to areas 17 and 18 of visual cortex. *Journal of Neurophysiology* **36**, 551–567.

STRYKER, M. P. & HARRIS, W. A. (1986). Binocular impulse blockade prevents the formation of ocular dominance columns in cat visual cortex. *Journal of Neuroscience* **6**, 2117–2133.

SUR, M., HUMPHREY, A. L. & SHERMAN, S. M. (1982). Monocular deprivation affects X- and Y-cell retinogeniculate terminations in cats. *Nature* **300**, 183–185.

SUR, M. & SHERMAN, S. M. (1982). Morphology of the terminal arborizations of physiologically identified X- and Y- retinal ganglion cell axons in the LGN_d of the cat. *Science* **218**, 389–391.

SUR, M., WELLER, R. & SHERMAN, S. M. (1984). Development of X- and Y-cell retinogeniculate terminations in kittens. *Nature* **310**, 246–248.

TOOTLE, J. S. & FRIEDLANDER, M. J. (1986). Postnatal development of receptive field surround inhibition in kitten dorsal lateral geniculate nucleus. *Journal of Neurophysiology* **56**, 523–540.

TOOTLE, J. S. & FRIEDLANDER, M. J. (1989). Postnatal development of the spatial contrast sensitivity of X- and Y-cells in the kitten retinogeniculate pathway. *Journal of Neuroscience* **9**, 1325–1340.

TSUMOTO, T. & SUDA, K. (1982). Laminar differences in development of afferent innervation to striate cortex neurones in kittens. *Experimental Brain Research* **45**, 433–446.

VAN ESSEN, D. C. (1982). Neuromuscular synapse elimination. In *Neuronal Development*, ed. SPITZER, N. C., pp. 333–376. New York: Plenum Press.

WIESEL, T. N. & HUBEL, D. H. (1963). Single cell responses in striate cortex of kittens deprived of vision in one eye. *Journal of Neurophysiology* **26**, 1003–1017.

WILSON, J. R., TESSIN, D. E. & SHERMAN, S. M. (1982). Development of the electrophysiological properties of Y-cells in the kitten's medial interlaminar nucleus. *Journal of Neuroscience* **2**, 562–571.

WINFIELD, D. A. (1981). The postnatal development of synapses in the visual cortex of the cat and the effects of eyelid closure. *Brain Research* **206**, 166–171.

WINFIELD, D. A. & POWELL, T. P. S. (1983). Laminar cell counts and geniculocortical boutons in area 17 of cat and monkey. *Brain Research* **277**, 223–229.